Plate tectonics and surface environment: Role of the oceanic upper mantle

Jun Korenaga

Department of Geology and Geophysics, Yale University, P.O. Box 208109, New Haven, CT 06520-8109, USA

jun.korenaga@yale.edu

Tel: (203) 432-7381; Fax: (203) 432-3134

Submitted to *Earth-Science Reviews*, December 2019.

Revised, March 2020.

Abstract. Earth is so far the only planet that exhibits plate tectonics, and along with the right heliocentric distance and the presence of surface water, plate tectonics is among necessary conditions for a habitable planet. Yet, the physics of this particular style of mantle convection is poorly understood, creating a substantial bottleneck in developing the general theory of planetary evolution. As plate tectonics is characterized by the subduction of oceanic lithosphere, a better understanding of the oceanic upper mantle could potentially help to break this stalemate. In this review, I summarize available theoretical, observational, and experimental constraints on the evolution of the oceanic upper mantle and its rheology, place the study of the oceanic upper mantle in the big picture of Earth evolution, and provide some suggestions for future research in relevant disciplines, including marine geophysics and computational geodynamics.

Keywords: marine geophysics, mantle rheology, numerical simulation

1 Introduction

Plate tectonics is what makes Earth a unique planet in the solar system (e.g., Rampino and Caldeira 1994; Schubert et al. 2001; Kasting and Catling 2003), but the physics of this particular style of mantle convection is still largely unresolved (e.g.. Bercovici et al. 2015). We still do not know, for example, under what conditions plate tectonics takes place on a terrestrial planet. The inability to answer this basic question creates a considerable bottleneck in developing the general theory of planetary evolution; such a theory would be invaluable for ongoing exoplanetary research, or more broadly speaking, our quest for the origins of life in the universe. As the defining characteristic of plate tectonics is the subduction of oceanic lithosphere, one promising direction is to improve our understanding of the oceanic upper mantle. To identify key issues that warrant further investigation, this paper provides a review on the role of the oceanic upper mantle in some major unresolved problems surrounding plate tectonics.

The oceanic upper mantle is perhaps the best understood part of Earth's mantle. To first order, its evolution is expected to be a simple function of seafloor age (e.g., Parsons and Sclater 1977; Stein and Stein 1992; Ritzwoller et al. 2004; Priestley and McKenzie 2013), and its chemical state is generally considered to be relatively homogeneous (e.g., Klein and Langmuir 1987; Hofmann 1997; Herzberg et al. 2007; Gale et al. 2014). The rheology of olivine, which is the dominant phase of the upper mantle, has been studied extensively (e.g., Chopra and Paterson 1984; Karato et al. 1986; Hirth and Kohlstedt 1995; Mei and Kohlstedt 2000a; Jung et al. 2006; Hansen et al. 2011). However, if we try to quantify how surface environment is controlled by mantle dynamics, it becomes evident that there exist a few major gaps in our understanding of the oceanic upper mantle. To keep discussion concrete in this paper, I will focus on the following three outstanding questions: (1) Why does plate tectonics take place on Earth? (2) How well can the surface topography of Earth, in the present and the past, be predicted? and (3) How does plate tectonics influence surface environment? To set the stage, I will first review the evolution of the oceanic upper mantle, covering thermal subsidence, seawater alteration, small-scale sublithospheric convection, perturbations by mantle plumes, the state of asthenosphere, and reference evolution models. Having a holistic view of mantle evolution is essential if we wish to correctly interpret any given observation, because real data reflect all of pertinent complications that exist in nature. Then, I will summarize available constraints on the rheology of the upper mantle materials, a good understanding of which is indispensable when discussing the dynamics of the oceanic upper mantle. With these preparations, I will return to the above outstanding problems and discuss how our understanding (or lack thereof) of the oceanic upper mantle contributes to ongoing debates over these issues. I will close with some suggestions for future research in relevant disciplines.

2 Evolution of the oceanic upper mantle

The generation of oceanic plates at mid-ocean ridges and their lateral migration are the directly observable part of global-scale mantle circulation. As a newly formed seafloor moves away from a mid-ocean ridge, it gradually cools down, becomes denser, and thus subsides. The first-order feature of seafloor topography, shallow mid-ocean ridges and deepening ocean basins, can be explained by the simple conductive cooling of the suboceanic mantle. As the characteristics of ocean basins are primarily determined by seafloor age, marine geophysical observations are often discussed in terms of "anomalies," i.e., deviations from some reference models. The evolution of the oceanic upper mantle, however, has some nontrivial complications, and a good understanding of how a 'normal' oceanic lithosphere would behave is necessary if we try to extract as much information as possible from a given observation by analyzing its subtle details.

In this paper, the terms "oceanic plate" and "oceanic lithosphere" both refer to the shallow, mechanically strong part of the oceanic mantle. The term "lithosphere" usually corresponds to the top thermal boundary layer, and this implicitly assumes that the mechanical strength of lithosphere originates in temperature-dependent viscosity. Viscosity can, however, depend on other factors such as grain-size and water content, and the precise definition of lithosphere becomes somewhat nebulous. In particular, mantle melting beneath mid-ocean ridges dehydrates the residual mantle, and this dehydration can lead to a substantial increase in viscosity (e.g., Karato 1986; Hirth and Kohlstedt 1996; Faul and Jackson 2007). In some contexts, it would be convenient to distinguish between "thermal lithosphere" and "chemical lithosphere" (which is made of crust and "depleted mantle lithosphere") (Figure 1); the former grows by conductive cooling from the above, whereas the latter is set by mantle melting beneath mid-ocean ridges. These two different types of lithosphere may eventually converge because the growth of a thermal boundary layer could be limited by the thickness of chemical lithosphere (Figure 1); i.e., when a thermal boundary layer becomes thicker than chemical lithosphere, eventual convective instability can remove the excess thickness (e.g., Korenaga and Jordan 2002b). The term "asthenosphere" is complementary to lithosphere, i.e., generally referring to a weak layer beneath lithosphere, so the ambiguity in the definition of lithosphere propagates to that of asthenosphere. Such ambiguity is natural to exist because it reflects how well we understand the mechanical properties of the mantle; our understanding is not so complete even for the oceanic upper mantle. Note that the "depleted mantle lithosphere" above is not the same as the "depleted mantle." The depleted mantle is a geochemical jargon referring to the mantle that is complementary to the continental crust (e.g., Hofmann 1988); i.e., the depleted mantle is depleted in incompatible elements compared to the primitive mantle because of the extraction of continental crust from the latter, and it refers to the present-day convecting mantle. The depleted mantle lithosphere is even more depleted because of the extraction of oceanic crust from the depleted mantle. This distinction is not always correctly made in the literature, and the reader is referred to section 2.4 of Korenaga (2017b) for a more complete explanation.

2.1 Seafloor subsidence

The majority of seafloor topography appears to follow thermal isostasy (Turcotte and Schubert 1982, section 4.23). With simple half-space cooling and constant material properties, the subsidence with respect to a zero-age seafloor, w, is given by

$$w = \frac{2\alpha\rho_m\Delta T}{\rho_m - \rho_w}\sqrt{\frac{\kappa t}{\pi}}, \quad (1)$$

where α is thermal expansivity, κ is thermal diffusivity, ρ_m is mantle density, ρ_w is water density, and ΔT is the difference between the surface temperature and the initial mantle temperature. Using $\alpha = 3 \times 10^{-5}$ K^{-1}, $\kappa = 10^{-6}$ m^2 s^{-1}, $\rho_m = 3300$ kg m^{-3}, $\rho_w = 1000$ kg m^{-3}, and $\Delta T = 1300$ K, the above equation may be expressed as $w \sim 355\sqrt{t}$, where t is in Ma and w in meters; e.g., 100-Ma seafloor would be ~3.55 km deeper than a mid-ocean ridge. However, explaining seafloor topography with this simplest kind of conductive cooling has at least two issues.

The first issue has long been known; actual seafloor depths start to deviated from the half-space cooling model for ages greater than ~80 Ma (Figure 2a). This deviation is known as "depth anomalies" or "seafloor flattening." Instead of half-space cooling, therefore, the so-called plate model is usually used to describe the age-depth relation of seafloor (Parsons and Sclater 1977; Stein and Stein 1992). The plate model can reproduce seafloor flattening because of its artificial boundary condition at ~100 km depth, which prevents the growth of the top thermal boundary layer beyond this depth. The depth of the boundary and its temperature are adjusted to fit the observed age-depth relation. The plate model itself is purely a phenomenological model, but there have been attempts to justify it in a physically sensible manner by calling for the possible occurrence of small-scale convection (Figure 1) (Parsons and McKenzie 1978; Davaille and Jaupart 1994; Dumoulin et al. 2001; Huang and Zhong 2005).

The second issue has become evident relatively recently, and this is about the younger part of seafloor (though it also concerns the older part indirectly). As noted above, the simple half-space cooling model yields the subsidence rate of ~355 m Ma$^{-1/2}$, and the subsidence of young (<80 Ma) seafloor had been thought to exhibit a similar rate (e.g., 350 m Ma$^{-1/2}$ by Davis and Lister (1974) and 345 m Ma$^{-1/2}$ by Carlson and Johnson (1994)). This apparent similarity between theory and observation turns out to be coincidental. The observed subsidence rate of young seafloor is likely to be $\sim$320$-$330 m Ma$^{-1/2}$ if we exclude the regions affected by the emplacement of anomalous crust (Korenaga and Korenaga 2008), whereas a more complete theoretical calculation of half-space cooling with variable material properties yields a subsidence rate of $\sim$500 m Ma$^{-1/2}$ (Korenaga and Korenaga 2016). Interestingly, this large gap between the observed and theoretical rates is also found to be consistent with the combined effects of various processes (other than conductive cooling) that should be operating within the oceanic mantle, including thermal cracking, radiogenic heat production, and secular cooling (Figure 2b).

Thus, how the depth of seafloor varies with its age is affected not only by the growth of a thermal boundary layer, and a better understanding of the age-depth relation must come with a more complete understanding of the evolution of the oceanic mantle as a whole, ranging from lithospheric processes (thermal cracking), through asthenospheric processes (small-scale sublithospheric convection), to mantle-wide processes (radiogenic heating and secular cooling). As will be discussed later in this section, recognizing this challenge is important when building a reference evolution model that can fit observations and is physically sensible.

2.2 Seawater alteration

Surface heat flow measured at young seafloor ($<$60 Ma) is noticeably lower than predicted by the cooling models of oceanic lithosphere (e.g., Stein and Stein 1994). As heat flow measurements are based on thermal conduction, this discrepancy in observed and predicted heat-flow values points to an important role of hydrothermal circulation in surface heat loss (Pollack et al. 1993; Jaupart and Mareschal 2015). Hydrothermal circulation can also chemically alter the shallow part of oceanic lithosphere, and the extent of seawater alteration is important for several major issues in earth system science, such as the redox evolution of the atmosphere (Holland 2002; Sleep 2005; Kasting 2013), global water cycle (Ito et al. 1983; Rüpke et al. 2004; Magni et al. 2014), and the secular evolution of seawater δ^{18}O (Wallmann 2001; Jaffres et al. 2007; Carmody et al. 2013). Despite this significance, it is still difficult to answer the following simple questions with confidence: how deeply seawater penetrates into oceanic lithosphere, and how much of the lithosphere is hydrated. The difficulty originates in the scarcity of decisive observational constraints and the immaturity of theoretical development.

Petrological and geochemical studies on ophiolites and contemporary oceanic crust can provide a cross-sectional view on the extent of seawater alteration (e.g., Gregory and Taylor 1981; Alt et al. 1986; Bickle and Teagle 1992; Dick et al. 2000), but most of ophiolites formed in supra-subduction settings (e.g., Miyashiro 1973; Searle and Cox 1999), and in situ sampling of oceanic crust by deep-sea drilling is still largely limited to upper-crustal sections (Gillis 1995; Wilson et al. 2006). The most extensive lower-crustal sample obtained by drilling has been a 1.5-km-long section from ODP Hole 735B in the Southwest Indian Ridge (Dick et al. 2000), but the success of drilling owes much to this section being tectonically exposed, so its state of alternation may not be representative of alternation in a typical oceanic lower crust. In both ophiolites and oceanic crust, the degree of alteration decreases with depths, though the penetration of hydrothermal fluids down to the mantle is also indicated by oxygen isotope data from the Oman ophiolite (Gregory and Taylor 1981; Stakes and Taylor 1992). The application of ophiolite-based inference to oceanic crust, however, requires caution because ophiolites are generally more extensively altered than oceanic crust (Alt and Teagle 2000).

Seawater alteration modifies the physical properties of rocks, so geophysical observations can potentially constrain the extent of hydration in oceanic lithosphere. By 20 % alteration, for example, the *P*-wave velocities of gabbro and peridotite decrease by $\sim$4 % (Carlson and Miller 2004) and $\sim$9 % (Christensen 2004), respectively (Figure 3). The *P*-wave velocity of oceanic lower crust is known to be $\sim$7 km s^{-1} (White et al. 1992), being lower than the velocity of unaltered gabbroic rocks ($\sim$7.3 km s^{-1} (Christensen and Smewing 1981)), which may indicate that $\sim$20 % of the lower crust is altered. However, such an interpretation is not unique (Korenaga et al. 2002; Behn and Kelemen 2003); crack-like porosity can lower seismic velocity quite easily with a minute amount of water involved (Figure 3). The alteration of gabbroic rocks by 20 % is equivalent to the water concentration of 0.35 wt%, and its effect on *P*-wave as well as *S*-wave velocities can be mimicked well by only 0.06 % porosity (0.02 wt% of water) if the porosity is crack-like, i.e., its aspect ratio (the ratio of the shorter semi-axis over the longer semi-axis of an oblate spheroid) is very small. Strangely, such effect of crack-like porosity has been largely neglected in the literature. Some authors try to justify the interpretation of seismic velocity anomalies in terms of alteration, by stating that the presence of cracks should facilitate the alteration of surrounding rocks (e.g., Carlson 2003; Ivandic et al. 2008), but large-scale cracks such as created by thermal cracking (Korenaga 2007b) are inefficient to promote hydration because of the effect of confining pressure on water transport (Korenaga 2017a). Canales et al. (2017) estimated the relation between *P*-wave velocity and water content based on the physical properties of drilled cores, but such an attempt would be valid only if large-scale cracks are absent.

A pair of *P*- and *S*-wave velocity models could potentially constrain the relative importance of alteration and crack-like porosity (e.g., Grevemeyer et al. 2018), but obtaining a reliable *S*-wave velocity model is difficult. This is because the identification of relevant *S* phases, such as *Sg*, *SmS*, and *Sn*, is often equivocal; they are all later phases, usually with low signal-to-noise ratios (see, for example, figure C2 of Contreras-Reyes et al. (2008)). Measuring electrical resistivity, which is sensitive to the volume of pore fluid, may help validate purely seismological inference, but such a joint analysis of seismic and electromagnetic data is still in its infancy (Naif et al. 2015).

It may be possible to predict how deeply oceanic lithosphere can be fractured and thus altered by seawater on the basis of numerical modeling, but numerical studies on the brittle deformation of oceanic lithosphere usually focus on large-scale faulting (e.g., Buck et al. 2005; Olive et al. 2010), and the consideration of thermal cracking is rare (Korenaga 2007b). Thermal cracking is likely to take a cascade structure (Lister 1974), in which narrowly-spaced shallow cracks and widely-spaced deep cracks coexist, and the evolution of such a complex multi-scale crack system is yet to be studied quantitatively.

It is important to appreciate the limitation of currently available observations and numerical models. An instructive example may be drawn from the recent literature on the hydration state of subducting slab. When bent at subduction zones, oceanic plates are fractured by normal faulting, and this bending-related faulting is widely believed to hydrate the lithosphere down to the depth of ∼20-30 km (e.g., Ranero et al. 2003). Being deeply faulted, however, does not guarantee deep hydration because of confining pressure; the buoyancy of water with respect to rocks acts to prevent the transport of water from faults into wall rocks. Though the modeling studies of Faccenda et al. (2009) and Dymkova and Gerya (2013) indicate that dynamic pressure associated with plate bending may be high enough to cancel confining pressure, such high dynamic pressure has been suggested to be at odds with a physical bound on the magnitude of dynamic pressure (Korenaga 2017a). Also, relevant geophysical observations do not seem to be compelling enough to challenge this theoretical constraint (Korenaga 2017a). When the possibility of crack-like porosity cannot be excluded, the interpretation of geophysical observations suffers from considerable nonuniqueness. Though it may not be widely appreciated (e.g., Hatakeyama et al. 2017; Cai et al. 2018), it is important to take into account the effect of confining pressure, which is significant at lithospheric scale, when discussing the state of mantle hydration.

2.3 Perturbations from within and below

As already discussed in section 2.1, the first order feature of seafloor topography can be explained by simple half-space cooling, i.e., the conductive growth of thermal boundary layer. At the same time, the steady growth of the boundary layer can be disrupted, sometimes quite substantially, both from within and below. The former corresponds to small-scale convection, and the latter to the impingement of mantle plumes.

Oceanic lithosphere is gravitationally unstable because the shallower part is colder and thus denser than the deeper part. Because of temperature-dependent viscosity, however, the coldest and densest part is too stiff to participate in convective instability, and only the lower portion can potentially be destabilized. When the instability develops into small-scale convection depends on mantle rheology. In general, convection takes place more easily for lower viscosity, and small-scale convection can start beneath very young (∼5 Ma) lithosphere if the viscosity of asthenosphere is as low as 10^{17}Pa s (e.g., Buck and Parmentier 1986). Such an early onset of convection was once suggested to be responsible for gravity lineaments observed on the young Pacific plate near the East Pacific Rise (Haxby and Weissel 1986), but based on subsequent geophysical and geochemical surveys, those lineaments are now considered to have resulted from the presence of chemical heterogeneities with low melting temperatures in the asthenosphere (Harmon et al. 2011), which facilitates melt-buoyancy-driven upwelling (e.g., Tackley and Stevenson 1993). The onset of small-scale convection, initiated by the destabilization of oceanic lithosphere itself, may be taking place beneath relatively mature (∼70 Ma) seafloor, as suggested by seismic tomography studies (e.g., Katzman et al. 1998; Ritzwoller et al. 2004). This timing happens to coincide with when seafloor subsidence deviates from the prediction of half-space cooling, lending some credibility to the small-scale convection origin of seafloor flattening (Parsons and McKenzie 1978). Because of the strongly temperature-dependent viscosity of the mantle, however, most of the lithosphere is too strong to be mobilized, and lithospheric thinning by convective delamination is limited (e.g., Solomatov 1995; Korenaga and Jordan 2003, 2004). Thus, even if small-scale convection takes place, additional mechanisms such as radiogenic heating are needed to explain the observed amplitude of seafloor flattening (Huang and Zhong 2005; Korenaga 2015b).

Seafloor flattening by small-scale convection could take place on a global scale when certain conditions for such intrinsic instability are met, e.g., lithosphere has grown sufficiently thick. By contrast, the impingement of a mantle plume can affect lithospheric evolution on a more regional scale and independently of the state of lithosphere. As the upwelling of a mantle plume is generally accompanied with extensive melting, its impingement on oceanic lithosphere is commonly believed to result in the formation of hotspot islands or an oceanic plateau, both of which are characterized by anomalously thick igneous crust (e.g., Morgan 1971; Richards et al. 1989; Coffin and Eldholm 1994). The thickness of such anomalous crust and its chemical composition can help constrain the physical and chemical state of a putative mantle plume (e.g., Watts et al. 1985; Caress et al. 1995; Hauri 1996; Sobolev et al. 2007; Richards et al. 2013), or more important, allows to assess the very assumption of a mantle plume (e.g., Sallares et al. 2005; Korenaga and Sager 2012). In addition to crustal emplacement, the impact of a mantle plume could also result in the thermal erosion of lithosphere (Sleep 1987; Ribe and Christensen 1994) as well as the spreading of buoyant residual mantle (Phipps Morgan et al. 1995; Ribe and Christensen 1999), contributing to broad seafloor shallowing around hotspot islands known as a hotspot swell. The amplitude of swell topography and its spatial extent are part of important constraints on the so-called plume buoyancy flux (Davies 1988; Sleep 1990; King and Adam 2014), which can be related to core heat flux.

The impact of mantle plumes on the evolution of oceanic lithosphere can vary substantially because the nature of mantle plumes is diverse (e.g., Courtillot et al. 2003; Foulger et al. 2005). The original concept of mantle plume, as proposed by Morgan (1971), is based on the upwelling of purely thermal anomalies, but such a simple notion has been shown to be inadequate to explain observations from quite a few hotspot islands and oceanic plateaus. Perhaps the most prominent example is the Ontong Java Plateau, the largest oceanic plateau found on the present-day seafloor (Coffin and Eldholm 1994). This plateau has >30-km-thick crust (Miura et al. 2004; Korenaga 2011b) and is believed to have formed on young seafloor, so if it was formed by the impact of a purely thermal plume, it is expected to have formed at least 1 km above sea level (Korenaga 2005b). However, the geological and geochemical analyses of drilled cores from the plateaus indicate that it was actually formed ∼1 km *below* sea level (Michael 1999; Mahoney et al. 2001; Roberge et al. 2005). The submarine eruption of Ontong Java Plateau thus exemplifies the difficulty of predicting the influence of a mantle plume on seafloor topography. Ontong Java Plateau may be a rare exception (other oceanic plateaus are much less explored), but it is by far the largest oceanic plateau, so this difficulty cannot be marginalized.

2.4 State of asthenosphere and its role in plate tectonics

As noted at the beginning of section 2, asthenosphere is complementary to lithosphere, the former being mechanically weaker than the latter. From the perspective of conductive cooling, asthenosphere represents merely the uncooled portion of the suboceanic mantle, and this simple picture is mostly sufficient to explain the long-wavelength features of relevant geophysical observations, e.g., the presence of the low velocity zone as seen in surface-wave tomography models (e.g., Ritzwoller et al. 2004; Debayle and Ricard 2012; Priestley and McKenzie 2013). In general, seismic velocities decrease with higher temperature and increase with higher pressure, and the combination of these competing effects creates a velocity minimum in the asthenosphere (e.g., Stixrude and Lithgow-Bertelloni 2005). However, finer structural details brought by body wave studies, such as the existence of the Gutenberg discontinuity and its magnitude (e.g., Kawakatsu et al. 2009; Rychert and Shearer 2011; Schmerr 2012), cannot be explained in a similar way because temperature and pressure vary only smoothly. There are two major hypotheses for the origin of the sharp seismic discontinuity, one with partial melting and the other with water. The partial melting hypothesis has a long history (e.g., Anderson and Sammis 1970; Ringwood 1975). The amount of partial melt expected from the thermodynamics of peridotites is quite small ($<$0.1 % (Hirschmann 2010)), but it may be sufficient to explain the strength of the Gutenberg discontinuity if the melt geometry is horizontally elongated (Kawakatsu et al. 2009; Takei 2017). The effect of water on seismic velocity could also be significant even with a trace amount of water (Karato 2012), though the efficacy of the proposed mechanism, i.e., anelastic relaxation by elastically accommodated grain boundary sliding, is yet to be explored (e.g., Cline et al. 2018).

Whereas the thermodynamics of a homogeneous peridotitic mantle predicts only a trace amount of partial melt ($<$0.1 %) in the asthenosphere, a much larger amount of partial melt can exist if the mantle is chemically heterogeneous (Hirschmann 2010). In fact, a chemically homogeneous mantle is too simple a concept to be realistic, and some degree of chemical heterogeneity is always expected from the operation of plate tectonics. In plate tectonics, the mantle is differentiated into oceanic crust and depleted mantle lithosphere by mid-ocean ridge magmatism, and these differentiated materials return to the mantle by subduction. Thus, plate tectonics constantly introduces chemical heterogeneities to the convecting mantle, and depending on the details of convective mixing (e.g., Olson et al. 1984; Manga 1996; Ferrachat and Ricard 1998), the fragments of subducted oceanic crust can persist as enriched heterogeneities, which can melt more easily than the surrounding peridotitic matrix (Yasuda et al. 1994). Local melt pockets originating in enriched chemical heterogeneities may be laterally elongated by shearing associated with mantle upwelling beneath mid-ocean ridges (Hirschmann 2010) (Figure 1), and such a melt geometry may explain th radial anisotropy of oceanic mantle (Kawakatsu et al. 2009) as well as the existence strong Po/So waves (suboceanic Pn/Sn phases) (Shito et al. 2013, 2015; Kennett et al. 2014). The presence of chemical heterogeneities should also manifest in the geochemistry of mid-ocean ridge basalts and ocean island basalts (e.g., Hirschmann and Stolper 1996; Ito and Mahoney 2005a, b; Sobolev et al. 2007; Gale et al. 2014), so by combining seismological and geochemical observations, we may be able to draw some unambiguous inferences on the nature of chemical heterogeneities in the suboceanic mantle. Such a multidisciplinary investigation is important because a chemically heterogeneous mantle is not a particularly well-defined notion and is often seen as an ad hoc explanation.

Even in the absence of enriched chemical heterogeneities, it is still possible to expect a locally high melt fraction beneath a relatively mature oceanic lithosphere if one considers the dynamic nature of the suboceanic mantle (e.g., Raddick et al. 2002; Ballmer et al. 2007). The convective instability of a growing lithosphere would cause the upwelling of asthenospheric mantle and its partial melting, and by vertical migration, melt can pond beneath the lithosphere, possibly reaching the melt fraction of a few percent. Ponded melt would eventually be solidified by a growing lithosphere, but the quasi-continuous presence of ponded melt may be achieved by the cycle of lithospheric delamination. In fact, the presence of such melt-rich lithosphere-asthenosphere boundary appears to be required by the fluid mechanics of petit-spot formation (Yamamoto et al. 2014). Petit-spot volcanos are tiny seamounts formed off the fore-bulge of the downgoing oceanic plate (Hirano et al. 2006), and even though their observable volumes are very small, their eruption through a thick mature oceanic lithosphere demands a robust supply of melt. Given the possibly ubiquitous presence of petit spots (e.g., Hirano et al. 2008, 2013), the effect of small-scale convection on the distribution of partial melt in the asthenosphere warrants careful quantification.

Apparently, it is widely believed that the presence of a low-viscosity layer beneath lithosphere is essential for plate tectonics (e.g., Sifre et al. 2014; Stern et al. 2015; Chantel et al. 2016; Takeuchi et al. 2017), and because of this, the presence of partial melt in the asthenosphere is often discussed as if it could control the likelihood of plate tectonics. There is no geodynamical basis for this belief. Of course, the viscosity of lithosphere is much higher than that of asthenosphere, because the former is colder than the latter. It is thus technically correct to say that plate tectonics is characterized by the presence of a low-viscosity layer beneath strong plates, but such characterization is not useful and can be misleading. What is most important for the persistent, long-term operation of plate tectonics is that, despite strongly temperature-dependent viscosity, lithosphere can become sufficiently weak, at least locally, to bend and subduct (e.g., Bercovici et al. 2015). Without such weakening of lithosphere, the style of mantle convection would be fixed to stagnant lid convection (Solomatov 1995), whether or not a low-viscosity layer exists. The overemphasis on the significance of a low-viscosity layer may originate in the earlier days of the plate tectonics revolution, in which plates were considered to float above the mantle and be driven by mantle convection (e.g., Isacks et al. 1968; Forsyth and Uyeda 1975). It could also stem from the work of Richards et al. (2001), whose numerical simulation indicates that the style of mantle convection is very sensitive to the presence of a low-viscosity layer (see their figure 4). Their conclusion, however, depends on their particular implementation of mantle rheology. As a number of other numerical studies demonstrate, it is the weakening of otherwise strong lithosphere, rather than the presence of a low-viscosity layer, that dictates the style of mantle convection (e.g., Stein et al. 2004; Landuyt et al. 2008; Stadler et al. 2010; Foley and Bercovici 2014). Also, if the viscosity of asthenosphere is too low, it would actually prevent the long-term operation of plate tectonics, because convective stress would be too low to break lithosphere (Solomatov 2004; Korenaga 2010). The lithosphere-asthenosphere system is an interesting test bed for our theoretical understanding of Earth's mantle, but it is also important to communicate its scientific merit correctly.

2.5 Reference evolution models and their significance

Observables related to oceanic lithosphere, such as seafloor depth, surface heat flow, and seismic velocity structure, are primarily a function of seafloor age, so it is natural to seek a reference evolution model, which can explain the first-order characteristics of the suboceanic mantle with simple physical principles. Such a reference model not only offers a concise summary of observables but also constrains the physical state such as thermal structure along with relevant material properties. The reference model also allows us to isolate deviations or anomalies, which can provide valuable constraints on dynamic processes that are distinct from large-scale mantle circulation.

Historically, there have been two approaches for how to define a reference model. One is to build a model based on the simplest physical assumption, i.e., the so-called half-space cooling (HSC) model (Turcotte and Oxburgh 1967; Davis and Lister 1974; Carlson and Johnson 1994). However sensible this approach may seem, the HSC model does not adequately explain the behavior of old ($>$80 My old) seafloor, as mentioned earlier in section 2.1. The other approach is to devise a phenomenological model that can fit observations, and the so-called plate model is the most popular in this category (McKenzie 1967; Parsons and Sclater 1977; Stein and Stein 1992). The major problem with this approach is that the model is constructed with a physically unrealistic boundary condition (constant temperature at a shallow ($\sim$100 km) depth). One may argue that such a boundary condition can be regarded as an approximation for physically plausible processes such as small-scale convection (e.g., Parsons and McKenzie 1978; Davaille and Jaupart 1994; Huang and Zhong 2005), but such an argument has been mostly qualitative. Whereas small-scale convection does help deviate from the prediction of the HSC model, thereby mimicking the behavior of the plate model, the thermal structure resulting from small-scale convection can be considerably different from that of the plate model (Figure 4).

The popularity of the plate model is understandable. The HSC model predicts simply too deep seafloor for old seafloor; the difference from the observed depth reaches as much as $\sim$1 km at the age of 140 Ma (Figure 2). At the same time, we should recognize that the plate model suffers from its use of a physically unrealistic boundary condition. The plate model was originally proposed to explain the roughly constant surface heat flow at old seafloor (Langseth et al. 1966; McKenzie 1967), and it is easy to explain this observation by imposing a constant temperature boundary condition at the depth of $\sim$100 km. However, the influence of such a boundary condition is not limited to the structure of old oceanic lithosphere; the influence may seem more subtle at young lithosphere (Figure 4), but it is actually substantial regarding seafloor subsidence (see Figure 4c of Korenaga and Korenaga (2016)). This is problematic. For young seafloor, the HSC model has no shortcomings, and if we extend the model with the possibility of small-scale convection, it can explain old seafloor as well (Huang and Zhong 2005; Korenaga 2015b). In this case, the thermal structure of oceanic lithosphere simply follows the prediction of half-space cooling until it is disturbed by small-scale convection. If we use the plate model, on the other hand, its bottom boundary condition inadvertently affects the thermal evolution of young lithosphere. In other words, the argument to justify this boundary condition as an approximation for the effect of small-scale convection (e.g., Parsons and McKenzie 1978) suffers from a causality problem. Small-scale convection taking place beneath old lithosphere cannot affect the thermal evolution of younger lithosphere.

Geoid data are sensitive to depth-integrated mass anomalies, and weak geoid contrasts observed on young seafloor across the Mendocino fracture zone were once suggested to prefer the thermal structure predicted by the plate model over that by the HSC model (Richardson et al. 1995), but this argument has been shown to be based on the incorrect theoretical calculation of geoid anomalies (Cadio and Korenaga 2012). On a more global scale, correlation between age and geoid slope was suggested to prefer the plate model (DeLaughter et al. 1999), but this argument is also tainted by the mishandling of theoretical calculations (Korenaga and Korenaga 2008). In general, the HSC model and the plate model predict similar geoid signals to each other, and the difference between them is much smaller than other perturbations expected in the geoid (Hager 1983). Surface wave tomography provides a more direct probe into the thermal structure of the suboceanic mantle, and a tomographic cross section stacked with respect to seafloor age commonly shows a continuous thickening of high velocity anomalies with age (Maggi et al. 2006; Debayle and Ricard 2012; Isse et al. 2019), which is more consistent with the HSC model than the plate model.

Thus, neither the (pure) HSC model nor the plate model is satisfactory; the former fails to account for the topography of old seafloor, whereas the latter is physically awkward. Even in the recent literature, however, it is still common to adopt the plate model despite its physical flaw because the HSC model cannot explain old seafloor (e.g., Goutorbe and Hillier 2013; Hoggard et al. 2017; Richards et al. 2018). It is probably time to quit such a banal dualistic argument and proceed in a more physically sensible direction. What is necessary is the third kind of reference model, which includes all of ubiquitous physical processes, i.e., not only half-space cooling but also other intrinsic processes for the suboceanic mantle such as thermal cracking, internal heating, secular cooling, and possibly even small-scale convection (Figure 1). According to preliminary attempts in this direction, it appears possible to build such a physics-based reference model that can fully account for the evolution of 'normal' oceanic lithosphere (Korenaga 2015b; Korenaga and Korenaga 2016).

The use of the qualifier 'normal' here is important; when constraining a reference model with observations, we should restrict ourselves to the part of suboceanic mantle that is devoid of perturbations from below (i.e., the impact of mantle plumes). Otherwise, we would not be able to quantify the influence of such perturbations accurately, and our understanding of normal suboceanic mantle would also be compromised. Traditionally, however, this issue tends to be handled arbitrarily. For example, Stein and Stein (1992) and Carlson and Johnson (1994) did not use any screening of seafloor when constructing their reference models. Some authors have tried to exclude seafloor presumably affected by mantle plumes, such as hotspot islands, seamounts, and oceanic plateaus, by visual inspection or similar semi-quantitative methods (Smith and Sandwell 1997; Hillier and Watts 2005). Others used more aggressive screening based on the distance from known hotspot tracks, e.g., >1000 km (Heestand and Crough 1981) and >600 km (Schroeder 1984), resulting in virtually no normal seafloor for ages greater than 80 Ma. Crosby et al. (2006) suggested that normal seafloor might be identified by near-zero gravity anomalies, but being in isostatic equilibrium does not necessarily mean being unaffected by perturbations from below; as an extreme case, consider Ontong Java Plateau, the majority of which is characterized by near-zero gravity anomalies (e.g., Coffin and Gahagan 1995). If the variation of oceanic crust thickness were globally known, such information could be used to extract the normal part of seafloor, but the current knowledge is far from being complete (e.g., Winterbourne et al. 2014). Moreover, as noted section 2.3, the impingement of a mantle plume would affect not only crustal thickness but also mantle lithospheric structure, so even a better understanding of global crustal structure is not sufficient. Given these considerations, there seems no better alternative, at the moment, than the spatial correlation approach (Korenaga and Korenaga 2008) to define normal seafloor. This approach requires only seafloor topography and is based on the notion that the influence of the emplacement of hotspot islands and oceanic plateaus on the surrounding seafloor should decrease with increasing distance from those anomalous regions. The quantification of this simple notion using spatial correlation has suggested that the influence of anomalous crust emplacement is statistically significant only up to the distance of $\sim$300 km (Korenaga and Korenaga 2008).

The potential benefit of a new kind of physics-based reference model, calibrated to normal seafloor, is multifold. First, it will allow a more accurate interpretation of geophysical data collected over normal seafloor (e.g., Sarafian et al. 2015; Lin et al. 2016; Baba et al. 2017; Takeo et al. 2018). This aspect is particularly important in light of the proposed Pacific Array (Kawakatsu and Utada 2017), an international effort to characterize the physical properties of the suboceanic mantle by global deployments of ocean-bottom seismometers and electromagnetometers. Second, it will help characterize anomalous regions with more confidence. Excess topography, for example, may indicate thicker-than-normal crust, thiner lithosphere, or the presence of thermally or chemically buoyant mantle below. As the plate model is tuned to fit the average behavior of old seafloor, a large fraction of old seafloor can be classified as 'normal' by definition, so the use of the plate model masks the potentially more anomalous nature of old seafloor. With a new reference model, it will be possible to better delineate how the evolution of oceanic lithosphere has been affected by perturbations from below. Lastly, unlike the purely phenomenological approach of the plate model, the physics-based approach can be extended to estimate the likely seafloor topography in the past. The shape of ocean basins is one of the most important components when quantifying the history of global water cycle and the emergence of dry landmasses (e.g., Korenaga et al. 2017). Developing a new reference model for the present-day suboceanic mantle can thus go a long way to become one of the pillars of the quantitative theory of Earth evolution.

3 Rheology of the oceanic upper mantle

The rheology of silicate rocks, i.e., how easily they deform under various conditions, is the most important unknown in mantle dynamics. The viscosity of mantle materials can vary over many orders of magnitude, but our current understanding does not allow us to prescribe how exactly it varies. In general, rocks become less viscous when heated up and more viscous when compressed. For olivine, which comprises $\sim$60 % of the upper mantle, we also know that olivine aggregates can deform by at least two different mechanisms, diffusion creep and dislocation creep; the former is sensitive to grain size, and the latter depends nonlinearly on stress. Deformation mechanisms are also known to be affected by chemical composition, and a trace amount of water can potentially reduce viscosity by a few orders of magnitude. However, when it comes to the details of such dependencies on temperature, pressure, grain size, stress, and composition, our understanding is still incomplete even for olivine, which is by far the best-studied mantle mineral. In this section, therefore, I review both experimental and observational constraints on upper mantle rheology. I will also discuss various numerical implementations of upper mantle rheology in the literature. Some implementations are more difficult to justify than others, and it is not uncommon to see questionable implementations even in widely-cited numerical studies. Understanding the rock-mechanics basis of common implementations helps us better evaluate the robustness of a certain suggestion based on numerical modeling. To make this section reasonably self-contained, I will start with some preliminaries of rock mechanics.

3.1 Preliminaries

When stains are large, rocks deform either in the brittle regime or in the ductile regime; the former is important under low temperatures and low pressures, and the latter under high temperatures and high pressures. In case of the oceanic upper mantle, both types of deformation are important. The brittle deformation regime *sensu lato* (i.e., including the brittle-ductile transition) is limited to relatively shallow depths, but it plays an important role in the strength of oceanic lithosphere, which is perhaps the most critical factor when discussing the plausibility of plate tectonics on terrestrial planets. The dynamics of the oceanic upper mantle influences that of the whole mantle. This is because the style of mantle convection is determined primarily by the nature of the top thermal boundary layer, i.e., whether oceanic lithosphere can subduct in case of Earth. Whether in the mode of plate tectonics or stagnant lid convection, how a terrestrial planet cools down boils down to the convective stability of the top thermal boundary layer, which determines surface heat flux. Thus, the rheology of the oceanic upper mantle holds a key to a variety of dynamical issues with a range of spatial and temporal scales.

The strength of rocks in the brittle deformation regime is often described in terms of yield strength as

$$\tau = \tau_0 + \mu P, \tag{2}$$

where τ_0 is the cohesive strength, μ is the friction coefficient, and P is pressure. The brittle strength of rocks depends on the size of intrinsic flaws, and larger samples would break more easily than smaller samples because the former can contain larger flaws (e.g., Jaeger and Cook 1976; Paterson and Wong 2005). The lowest possible brittle strength can be derived by considering pervasively fractured rocks, the strength of which is determined solely by frictional resistance along preexisting faults (e.g., Scholz 2002). Equation (2) represents such a lower bound on brittle strength. Laboratory experiments indicate that the friction coefficient is ∼0.6-0.85 for a wide variety of lithologies and the cohesive strength is negligible (Byerlee 1978). Note that Byerlee (1978) derived two empirical fits for his experimental data: (1) $\tau_0 = 0$ and $\mu = 0.85$ for data with confining pressures lower than 200 MPa, and (2) $\tau_0 = 50$ MPa and $\mu = 0.6$ for data with greater pressures, but this does not mean that the cohesive strength can be as high as 50 MPa. The use of two empirical fits is to represent the variation of friction coefficient with confining pressure with simple straight line fit (Byerlee 1978). The use of high cohesive strength (i.e., the depth-independent part of brittle strength) in the numerical simulation of mantle convection is common (e.g., Moresi and Solomatov 1998; Richards et al. 2001; O'Neill et al. 2007; Nakagawa and Tackley 2012), but it has no experimental support. As indicated by equation (2), brittle strength increases linearly with depth (or equivalently, pressure), and it becomes substantial even at moderate depths; with μ=0.8, for example, it reaches ∼1 GPa at the depth of 30 km. It may be possible to regard the depth-independent brittle strength as an effective, depth-average brittle strength, but whether or not the brittle strength depends on depth turns out to be important for the style of mantle convection (e.g., Moresi and Solomatov 1998) (see also section 3.5).

When multiple deformation mechanisms are available, rocks deform predominantly by the mechanism that provides the lowest yield strength. Therefore, whereas the brittle strength continues to increase with depth, brittle deformation eventually becomes irrelevant when ductile deformation becomes more effective. Olivine is the key mineral for upper mantle rheology, because it is the most abundant and usually the weakest phase among upper mantle minerals (e.g., Karato and Wu 1993). For the ductile deformation of olivine aggregates, the following four mechanisms have been suggested to be important: low-temperature plasticity, diffusion creep, dislocation creep, and dislocation-accommodated grain boundary sliding (GBS) (e.g., Goetze 1978; Karato and Wu 1993; Hirth and Kohlstedt 2003). Ductile deformation is usually described by a flow law, and each of these mechanisms is described by a different form of flow law. Also, each mechanism is known to require two different flow laws, one for deformation under dry conditions and the other under wet conditions (e.g., Karato et al. 1986; Mei and Kohlstedt 2000a, b; Katayama and Karato 2008; Ohuchi et al. 2015). Thus, fully describing the ductile deformation of olivine aggregates requires at least the following eight flow laws:

$$\dot{e}_{\mathrm{ltp,dry}} = A_1 \sigma^2 \exp\left(-\frac{E_1 + PV_1}{RT}\left[1 - \left\{\frac{\sigma}{\sigma_1}\right\}^{p_1}\right]^{q_1}\right) \quad (3)$$

$$\dot{e}_{\mathrm{ltp,wet}} = A_2 C_w^{r_2} \sigma^2 \exp\left(-\frac{E_2 + PV_2}{RT}\left[1 - \left\{\frac{\sigma}{\sigma_2}\right\}^{p_2}\right]^{q_2}\right) \quad (4)$$

$$\dot{e}_{\mathrm{diff,dry}} = A_3 d^{-m_3} \sigma \exp\left(-\frac{E_3 + PV_3}{RT}\right), \quad (5)$$

$$\dot{e}_{\mathrm{diff,wet}} = A_4 C_w^{r_4} d^{-m_4} \sigma \exp\left(-\frac{E_4 + PV_4}{RT}\right), \quad (6)$$

$$\dot{e}_{\mathrm{dis,dry}} = A_5 \sigma^{n_5} \exp\left(-\frac{E_5 + PV_5}{RT}\right), \quad (7)$$

$$\dot{e}_{\mathrm{dis,wet}} = A_6 C_w^{r_6} \sigma^{n_6} \exp\left(-\frac{E_6 + PV_6}{RT}\right), \quad (8)$$

$$\dot{e}_{\mathrm{gbs,dry}} = A_7 d^{-m_7} \sigma^{n_7} \exp\left(-\frac{E_7 + PV_7}{RT}\right), \quad (9)$$

$$\dot{e}_{\mathrm{gbs,wet}} = A_8 C_w^{r_8} d^{-m_8} \sigma^{n_8} \exp\left(-\frac{E_8 + PV_8}{RT}\right), \quad (10)$$

where $\dot{e}$ is strain rate (the subscript "ltp" for low-temperature plasticity, "diff" for diffusion creep, "dis" for dislocation creep, "gbs" for GBS, and "dry" and "wet" denote the absence and presence of water, respectively), σ is the second invariant of the deviatric stress tensor, T is temperature, P is pressure, R is the universal gas constant, d is grain size, C_w is water content, and A_i, E_i, V_i, σ_i, m_i, n_i, and r_i are, respectively, the pre-exponential factor, the activation energy, the activation volume, the Peierls stress, the grain-size exponent, the stress exponent, and the water-content exponent for the ith flow law (e.g., Karato 2008). The exponents p_i and q_i are constants with the range of $0 \leq p_i \leq 1$ and $1 \leq q_i \leq 2$ (e.g., Frost and Ashby 1982). Thus, the flow-law parameters that have to be determined experimentally include: eight A_i's, eight E_i's, eight V_i's, two σ_i's, two p_i's, two q_i's, four m_i's, four n_i's, and four r_i's, amounting to 42 unknowns in total. As explained later (section 3.3), many of these parameters are not well constrained, but in general, the ductile deformation is very sensitive to temperature, and at temperatures higher than ∼700 °C, the mantle deforms predominantly in the ductile regime. Through activation volume V_i, ductile deformation also depends on pressure, but the effect of pressure is moderate under upper mantle pressures. Thus, brittle and ductile deformation mechanisms are contrasting in their temperature and pressure dependence; the former depends strongly on pressure but is largely insensitive to temperature, and the opposite is true for the latter.

Experimental studies also suggest the existence of the semi-brittle regime (Kohlstedt et al. 1995), but our understanding of this intermediate regime is limited. It is common to assume, based on laboratory observations, that this regime is initiated when plastic flow strength is about five times the frictional strength (called brittle-ductile transition (BDT)) and is terminated when the lithostatic pressure exceeds the flow strength (brittle-plastic transition (BPT)) (Kohlstedt and Mackwell 2009; Mei et al. 2010). Without theoretical underpinning, it is difficult to evaluate the validity of such an empirical approach to lithospheric-scale problems. Future progress on the physics of brittle-ductile transition is much needed (e.g., Chester 1995; Aharonov and Scholz 2019).

3.2 Strength of oceanic lithosphere

The strength of oceanic lithosphere can be quantified by assessing the relative significance of these various deformation mechanisms as discussed above. For this purpose, a yield stress envelope is often used (Goetze and Evans 1979; Kohlstedt et al. 1995). Yield stress or yield strength refers to the maximum differential stress that can be supported by the type of rocks under consideration (olivine aggregates in case of oceanic lithosphere), and the envelope shows how yield stress varies with depth (Figure 5). For brittle deformation, equation (2) or its variant is used. For ductile deformation, a flow law is solved for stress by specifying other variables, such as pressure, temperature, and strain rate. Pressure is determined by depth, and by assuming a certain age for oceanic lithosphere, temperature can also be calculated as a function of depth (e.g., by using the half-space cooling model). For strain rate, the value of 10^{-15} s^{-1} is typically used. This value, often referred to as "the geological strain rate," corresponds to a representative strain rate in geological processes including mantle convection. For example, shearing the whole mantle by plate motion at the rate of 10 cm yr^{-1} (as in the case of the Pacific plate) and doubling crustal thickness within 30 Myr (as in the building of the Himalayas by the collision of the Indian subcontinent) are both characterized by the strain rate of $\sim 10^{-15}$ s^{-1}.

From the yield stress and the assumed strain rate, we can also calculate effective viscosity as

$$\eta_{\text{eff}} = \frac{\sigma_{\text{yield}}}{\dot{e}}. \tag{11}$$

For the geological strain rate of 10^{-15} s^{-1}, the yield stress of 100 MPa, for example, corresponds to the effective viscosity of 10^{23} Pa s (Figure 5b).

Figure 5a shows a yield strength envelope for 60-Ma oceanic lithosphere (thick gray line). Using the logarithmic scale for yield strength (Figure 5b) helps better understand the details of how such an envelope is constructed. First, as noted earlier, the brittle-ductile transition is defined where plastic flow strength is about five times the frictional strength (indicated by horizontal arrow in Figure 5b); such a crossover takes place at $\sim$2 GPa, which is out of the scope in a typical yield strength diagram (e.g., Figure 5a). The brittle-plastic transition takes place where the lithostatic pressure exceeds the flow strength, and low-temperature plasticity plays a key role in both transitions, as it provides the lowest yield strength among plastic deformation mechanisms. For 60-Ma oceanic lithosphere, and with the chosen flow-law parameters for this example, low-temperature plasticity is taken over at $\sim$60 km depth by dislocation creep, which in turn is taken over at $\sim$80 km depth by diffusion creep. Here the yield strength takes the maximum of 800 MPa at $\sim$25 km depth, and the substantial strength (>100 MPa) is maintained up to ∼50 km depth. It is well known, based on a number of numerical simulation studies (e.g., Moresi and Solomatov 1998; Richards et al. 2001; Stein et al. 2004), that such high yield strength does not allow the operation of plate tectonics.

As plate tectonics is currently taking place on Earth, however, there must be some weakening mechanism(s) that can reduce the yield strength of oceanic lithosphere, at least locally. The so far proposed weakening mechanisms that are consistent with rock mechanics include grain-size reduction (e.g., Kameyama et al. 1997; Braun et al. 1999; Landuyt et al. 2008; Bercovici and Ricard 2012) and thermal cracking (Korenaga 2007b). The idea of grain-size reduction has been motivated by the common occurrence of fine-grained rocks called mylonites in plate boundaries (e.g., Kirby 1985; Drury et al. 1991). One appealing aspect of grain-size reduction is that it could lead to strain localization by positive feedback; deformation through dynamic recrystallization reduces grain size, which promotes further deformation with grain-size-sensitive creep. This localization feedback is, however, usually considered to be limited because dynamic crystallization takes place when deformation takes place in the dislocation creep regime, whereas deformation is sensitive to grain size in the diffusion creep regime. That is, dynamic recrystallization cannot reduce grain size indefinitely because a system with too small grains would deform by diffusion creep, which does not cause dynamic recrystallization. Recent experimental and theoretical studies have delineated the details of how grain-size reduction proceeds by the interaction between dynamic recrystallization and phase mixing (e.g., Linckens et al. 2014; Cross and Skemer 2017; Bercovici and Skemer 2017), and because a considerable strain is required for such an interaction to become effective, the formation of fine-grained rocks is suggested to be a consequence, as opposed to the cause, of shear localization.

Even if grain-size reduction takes place quickly, however, its effect on lithospheric strength is still limited to the relatively warm part of oceanic lithosphere (>600 °C), as can be seen by comparing Figure 5b (reference yield strength envelope) and Figure 5c (that with a grain size of 100 μm). Even with a grain size of 100 nm, the strongest part of the lithosphere (<400 °C) is virtually unaffected. When the effect of grain-size reduction is considered in the numerical studies of mantle convection (e.g., Landuyt et al. 2008; Foley et al. 2014), this limited effect of grain-size reduction is usually relieved by introducing additional assumptions on lithospheric strength (see section 3.5).

Compared to grain-size reduction, thermal cracking is much less understood, though its possible role in large-scale lithospheric dynamics was already mentioned in the early 1970s (Turcotte and Oxburgh 1973). Thermal cracking can happen when thermal stress, resulting from thermal contraction, exceeds material strength, and it can take place over a range of scales, from the grain scale, owing to the anisotropy of thermal expansion of constituent minerals (e.g., Simmons and Richter 1976; Kranz 1983), to the lithospheric scale, owing to the isotropic component of thermal expansion (e.g., Turcotte 1974; Gans et al. 2003; Sandwell and Fialko 2004). Whereas grain-scale microcracks are likely to be closed by lithostatic pressure at depths greater than a few kilometers (e.g., deMartin et al. 2004), large-scale thermal cracks can remain open even at greater depths with sufficiently high thermal stress (e.g., Lachenbruch 1961). With a linear thermal expansivity of 10^{-5} K^{-1}, a bulk modulus of 100 GPa, and a temperature drop of 1000 K, thermal stress can be on the order of 1 GPa. When applied to the cooling of oceanic lithosphere, theoretical calculations suggest that thermal cracking could result in a cascade crack system characterized by narrowly spaced shallow cracks and widely spaced deep cracks (Korenaga 2007b). Thermal cracking in the presence of surface water leads to serpentinization of wall rocks, but as mentioned in section 2.2, serpentinization is limited to shallow depths, trapping water in deep crack by sealing surface openings. Though the total volume of solids and water is reduced by serpentinization, the sealing of surface openings is still possible because serpentinization at shallow depths is a chemically open system, i.e., seawater can freely move in and out. Because such trapped water could reduce the effective friction coefficient, especially when tectonically compressed, thermal cracking can potentially remove the strongest part of lithosphere altogether (Korenaga 2007b), lowering the maximum yield strength down to $\sim$100 MPa (Figure 5d).

The efficacy of thermal cracking is sometimes questioned because it does not crack lithosphere all the way (e.g., Bercovici et al. 2015), and indeed, the calculations of Korenaga (2007b) indicate that thermal cracking is effective only for temperatures below ∼700 °C. Above ∼700 °C, however, low-temperature plasticity happens to become the weakest deformation mechanism; i.e., thermal cracking is maximally effective in reducing lithospheric strength. This coincidence of thermal cracking and low-temperature plasticity occurs at all lithospheric ages; see Figure 7 of Korenaga (2018) for the cases of 30 Ma and 100 Ma. Unlike grain-size reduction, thermal cracking is not associated with any shear-localizing feedback, and because of this, thermal cracking appears unpopular among those who regard such a feedback as the essential weakening mechanism (e.g., Bercovici et al. 2015). As thermal cracking directly creates the localized zones of weakness, however, such a feedback may not be essential.

Thus, the colder and warmer parts of oceanic lithosphere may be weakened by different mechanisms: thermal cracking for the former and grain-size reduction for the latter. This is still a tentative summary, because the yield strength envelopes shown in Figure 5 are based on the combination of multiple deformation mechanisms, all of which suffer from substantial uncertainties. There are two clear tasks in front of us. One is to understand the current limitation of experimental constraints and explore new ways to improve them. The other is to test our understanding of experimental rock mechanics, which are necessarily based on deformation at microscopic scales, at lithospheric scales by some geophysical observations. A related issue is how to cope with the continuing uncertainties of mantle rheology when conducting geodynamical modeling. These issues will be discussed next in turn.

3.3 Experimental constraints

As described in section 3.1, we need up to eight flow laws (equations (3)-(10)) just to describe the ductile deformation of olivine aggregates, and these equations contain 42 unknown parameters in total. Most of these parameters are not well constrained owing to fundamental experimental limitations. First of all, typical strain rates achieved in deformation experiments are on the order of 10^{-5} s^{-1}, i.e., ten orders of magnitude faster than the geological strain rate. The strain rate of 10^{-5} s^{-1} is needed to conduct experiments on human timescales. Thus, using an experimentally-determined flow law always involves extrapolation over ten orders of magnitude, which underscores the importance of understanding how accurately the flow law is constrained; a seemingly small uncertainty in flow-law parameter could have a devastating effect when extrapolated to mantle conditions. To deform rocks at the strain rate of 10^{-5} s^{-1}, experiments are usually conducted at high temperatures and high stresses and with very small grain sizes, and it is difficult to deviate from this usual practice. For example, the range of temperature used for the deformation of olivine aggregates is typically from 1425 K to 1575 K (e.g., Karato et al. 1986; Mei and Kohlstedt 2000a; Hansen et al. 2011); i.e., the activation energy, which measures temperature dependence, is constrained by the span of only 150 K. Higher temperatures would cause partial melting, and lower temperatures would lead to too small a strain rate to be measured. Also, a number of deformation experiments were conducted at low pressures ($<$400 MPa, equivalent to $\sim$12 km depth), because the accurate measurement of deviatoric stress becomes impossible at higher pressures with a typical gas-medium deformation apparatus. Recent technical development, combined with the use of synchrotron X-ray radiation, has allowed deformation experiments at much higher pressures (a few GPa) (Kawazoe et al. 2009; Durham et al. 2009), but deviatoric stresses in such high-pressure experiments are also very high ($\sim$1 GPa), being a few orders of magnitude greater than stresses associated with mantle convection.

In addition to these experimental limitations, there also exists an entirely different kind of difficulty when estimating flow laws from deformation data. Rock deformation under laboratory conditions is typically associated with multiple deformation mechanisms (Karato 2010). When estimating flow-law parameters based on deformation data, therefore, we need to deconvolve different mechanisms at the same time. Estimating the parameters of multiple flow laws simultaneously is a highly nonlinear inverse problem, the proper treatment of which has become possible only in recent years (Korenaga and Karato 2008). A series of recent reanalysis of well-known deformation experiments on olivine single crystals and aggregates have brought rather unsettling findings. First, the stress exponent of dislocation creep, which was considered to be tightly constrained at 3.5 (Bai et al. 1991), has been shown to be more variable, from $\sim$2 to $\sim$5 (Mullet et al. 2015). Second, the conventional way of estimating flow-law parameters from individual experimental runs is found to provide only marginally useful estimates (Jain et al. 2018). Most recently, a global inversion of published deformation data, i.e., a simultaneous inversion of multiple experimental runs with inter-run biases taken into account, has provided a set of flow-law parameters (Jain et al. 2019), many of which are noticeably different from previous compilations (Karato and Wu 1993; Hirth and Kohlstedt 2003). As Table 1 shows, the grain-size exponent is $\sim$2 for diffusion creep as opposed to the frequently assumed value of 3, and the stress exponent for dislocation creep is $\sim$4.5 under wet conditions. The activation energy for dry dislocation creep is lower than previous estimates by $\sim$100 kJ mol^{-1}. Under dry conditions, The activation volume is not constrained by existing data, and even under wet conditions, it is only loosely constrained. There have been a large number of geodynamical studies that have adopted the flow-law parameters of either Karato and Wu (1993) or Hirth and Kohlstedt (2003) literally at face value, but the comparison of these two widely-cited compilations with the latest estimate by Jain et al. (2019) undermines the rock-mechanical basis of such studies.

Besides diffusion and dislocation creep, GBS has also been frequently discussed as an important rate-limiting deformation mechanism at high temperatures (Hirth and Kohlstedt 2003; Faul and Jackson 2007; Hansen et al. 2011; Ohuchi et al. 2015). However, the aforementioned global inversion by Jain et al. (2019) suggests that GBS plays only a minor role even under laboratory conditions and that it becomes almost irrelevant under mantle conditions.

Low-temperature plasticity, which controls the strength of the coldest part of lithosphere, has received a renewed interest in the last decade or so (e.g., Kawazoe et al. 2009; Mei et al. 2010; Long et al. 2011; Proietti et al. 2016; Kumamoto et al. 2017), and some of those recent studies suggest that low-temperature plasticity may lead to considerably weaker lithosphere than previously thought. Based on the numerical modeling of dislocation dynamics, Idrissi et al. (2016) have suggested the following flow-law parameters for equation (3): $A_1 = 1 \times 10^6$, E_1=566 kJ mol^{-1}, σ_1=3.8 GPa, p_1=1/2, and q_1=2 (note: the σ^2 and PV_1 terms are not considered in their study), and this flow law predicts lithospheric yield strength considerably lower than indicated in Figure 5. Subsequently, Kumamoto et al. (2017) suggested, given the possibility of the grain-size dependency of low-temperature plasticity, the flow law of Idrissi et al. (2016) is the best available for capturing the strength of coarse-grained mantle at low temperatures. However, this suggestion is debatable on several accounts. First, the grain-size dependence of low-temperature plasticity, as summarized by Figure 4 of Kumamoto et al. (2017), does not explain the experimental data of Proietti et al. (2016), which is of the smallest grain size among the data compiled by them. Also, their suggested trend of grain-size dependence relies heavily on the data of Druiventak et al. (2011), which is of the largest grain size in the compilation, but as can be seen from Figure 9 of Druiventak et al. (2011), almost all of their data fall on the trend defined by models of brittle failure (Byerlee's law or Goetze criterion), showing nearly linear increase in strength with confining pressure. More important, the flow law of Idrissi et al. (2016) is in gross conflict with existing experimental data (Figure 6). The deformation of coarse-grained ($\sim$900 μm) natural dunite samples at the stress of $\sim$0.5 GPa and the temperatures of $\sim$1500 K is on the order of 10^{-4} s^{-1} (Chopra and Paterson 1984), but the strain rate predicted by the flow law of Idrissi et al. (2016) is two orders of magnitude greater. In other words, their flow law is effective even at high temperatures. The deformation data of Chopra and Paterson (1984) fall almost completely in the regime of dislocation creep, so contributions from low-temperature plasticity must be negligible (i.e., with strain rate at least a few orders of magnitude lower). Therefore, whereas the low-temperature plasticity of olivine aggregates might depend on grain size, such dependency is likely to be considerably weaker than suggested by Kumamoto et al. (2017). In fact, a more recent study by Hansen et al. (2019) shows a negligible effect of grain size on *steady-state* deformation in the regime of low-temperature plasticity; the effect of grain size appears to be limited to transient creep, which is beyond the scope of equation (3).

To understand the extent of experimental constraints on low-temperature plasticity, Jain et al. (2017) reanalyzed the high-pressure deformation data of Mei et al. (2010) with a comprehensive inverse approach, and they found that existing experimental data could not uniquely determine the exponents p_1 and q_1 in equation (3), and that the yield strength prediction based on low-temperature plasticity depends strongly on the assumed values for those exponents, with the choice of $p_1 = q_1 = 1$ giving the weakest lithosphere. This particular choice of exponents, however, corresponds to a case of discrete-obstacle control (Frost and Ashby 1982), which is probably inappropriate for olivine; a material with strong chemical bonding usually has high Peierls stress, and in such a material, the intrinsic resistance of a dislocation against glide is likely to be more important. For this reason, the case of $p_1 = 1$ and $q_1 = 2$, which predicts the second weakest lithospheric strength (Jain et al. 2017), is adopted for the flow-law parameters of low-temperature plasticity in this paper (Figure 5).

Thus, even though the rheology of olivine has been investigated more extensively than that of any other mantle minerals, the currently available experimental constraints suffer from substantial ambiguity. Needless to say, more experimental data will be necessary. At the same time, a rigorous statistical analysis of rock deformation data must become part of standard analysis in the experimental community. Bayesian inversion based on Markov chain Monte Carlo, which is the basis of the aforementioned reanalyses, is still time-consuming, but it would not be overwhelmingly so if we wish to maximize the scientific merit of future experimental work.

3.4 Observational constraints

On a global scale, the viscosity structure of Earth's mantle has long been estimated based mostly on postglacial rebound and the long-wavelength geoid (e.g., Hager 1991; King 1995; Kaufmann and Lambeck 2000; Mitrovica and Forte 2004; Rudolph et al. 2015). Such a global estimate is radially symmetric (i.e., suboceanic and subcontinental regions are averaged) and provides only a crude view of likely viscosity stratification, typically with the following three parts: strong lithosphere, weak asthenosphere, and more viscous lower mantle. Thus, more detailed information about the rheology of oceanic upper mantle, such as how yield strength varies within the lithosphere, must come from more regional approach.

Estimating viscosity from geophysical observations is generally difficult. The most straightforward way would be just to divide stress by strain rate if we can estimate both, but having both estimates is rare. As the mantle can flow only very slowly, a reasonably accurate estimate on strain rate requires a record of long-term deformation. A rare example is postglacial rebound, which is an isostatic adjustment of landmasses formerly depressed by ice sheets; it is about deformation over 10^4 years, and the driving stress for this deformation can be estimated from surface topographic variations. One caveat on postglacial-rebound based estimates is that the associated strain is on the order of 10^{-3}, which is too small to achieve steady-state deformation. Laboratory experiments show that strains of $\sim$0.01–0.1 are necessary to achieve steady-state deformation (e.g., Karato et al. 1986; Hansen et al. 2019). Postglacial rebound data are thus useful to constrain transient creep, not steady-state creep (Karato 1998). It is always important to understand what kind of rheology is relevant to a given geophysical observation.

These difficulties, i.e., identifying appropriate observations, ideally with long-term deformation, and interpreting them with proper rheological models, persist when estimating the rheology of oceanic upper mantle. For the rheology of oceanic lithosphere, lithospheric flexure due to seamount loading is promising as it reflects deformation over 10^4-10^8 years (Watts 2001). Early interpretations of seamount loading history were made in the framework of temperature-dependent Newtonian viscosity (similar to equation (5)); Courtney and Beaumont (1983) suggested the activation energy of 170-250 kJ mol^{-1} with the asthenospheric viscosity of 10^{19}-10^{20} Pa s, and Watts and Zhong (2000) concluded similarly. Lithospheric flexure, however, involves multiple deformation mechanisms (Goetze and Evans 1979; see also Figure 5), the collective behavior of which may not be approximated well by temperature-dependent viscosity. More recently, Zhong and Watts (2013) investigated lithospheric deformation by the loading of the Hawaiian Islands, using finite-element modeling incorporating Byerlee's law, low-temperature plasticity, and high-temperature creep, and they suggested that laboratory-based flow laws for low-temperature plasticity predict too strong lithosphere to be compatible with observations. This may be consistent with the possibility of thermal cracking reducing the lithospheric strength (compare Figures 5b and 5d).

For the rheology of the warmer part of oceanic upper mantle, inferences based on convective instability are common. For example, based on the notable thinning of oceanic lithosphere at $\sim$70 Ma in their seismic tomographic model, Ritzwoller et al. (2004) suggested the asthenospheric viscosity of 4×10^{19} Pa s with the activation energy of 120 kJ mol^{-1}. The lithospheric thinning of such extent is, however, not seen in later tomographic models (e.g., Maggi et al. 2006; Debayle and Ricard 2012; Isse et al. 2019). As discussed in section 2.3, the onset of small-scale convection at $\sim$70 Ma seems to be consistent with the record of seafloor subsidence, but the amplitude of seafloor flattening alone does not uniquely constrain asthenospheric viscosity and activation energy (Korenaga 2015b).

Besides old seafloor, beneath which thick lithosphere can become convectively unstable, a fracture zone is another locus for lithospheric instability because substantial lateral temperature variations across a fracture zone can facilitate the onset of small-scale convection (Huang et al. 2003). Cadio and Korenaga (2014) developed a new geoid inversion scheme to constrain density anomalies in the shallow mantle, and based on its application to geoid anomalies around major fracture zones in the Pacific, Cadio and Korenaga (2016) identified numerous small-scale density anomalies, which require temperature contrast of $\sim$300 K. If such anomalies result from the convective delamination of oceanic lithosphere, the scaling of Solomatov and Moresi (2000) indicates that the activation energy of temperature-dependent viscosity has to be as low as 100 kJ mol^{-1} for the case of diffusion creep and 225 kJ mol^{-1} for dislocation creep (assuming the stress exponent of 3.5), both of which are considerably lower than laboratory-based estimates (Table 1). At the moment, the cause of this discrepancy remains unclear.

Another type of dynamics-related inference is based on interpreting heat flow at old ocean floor using the scaling law derived for steady-state sublithospheric convection (Davaille and Jaupart 1994; Doin et al. 1997; Dumoulin et al. 1999; Solomatov and Moresi 2000), providing estimates on asthenospheric viscosity in the range of 10^{18}-10^{19} Pa s. Even if small-scale sublithospheric convection takes place, it is not clear whether such convection has reached a steady state beneath old seafloor (Korenaga and Jordan 2002a). A scaling derived by Korenaga (2009) suggests that the time scale to achieve steady-state convection is $\sim 8 \pm 2$ times greater than the onset time of convection, so if small-scale convection initiates at 70-Ma seafloor, then it would take another $\sim$300-600 Myr to reach a steady state.

Other estimates on the viscosity of suboceanic mantle are not directly related to steady-state creep. For example, by applying the Maxwell frequency scaling of McCarthy et al. (2011) to the seismic tomographic models of the Pacific upper mantle, Priestley and McKenzie (2013) estimated the activation energy of $\sim$400 kJ mol^{-1} and the activation volume of $\sim$8 cm^3 mol^{-1}. These estimates are comparable with laboratory-based estimates (Table 1), but with these temperature and pressure dependence, their estimate of reference viscosity (2×10^{22} Pa s, defined at 1473 K and 1.5 GPa) is equivalent to the asthenospheric viscosity of $\sim 6 \times 10^{21}$ Pa s (when evaluated at 200 km depth). This inference relies on the assumption that the scaling of McCarthy et al. (2011) is valid for all relevant frequencies, which has been questioned by subsequent experiments (Takei et al. 2014; Yamauchi and Takei 2016). Also, microscopic processes responsible for anelasticity (and thus seismic velocity) and those for long-term creep could be different (Karato et al. 2015).

In recent years, a growing number of viscosity estimates have been published for the sub-oceanic mantle, based on the analyses of postseismic deformation data (e.g., Panet et al. 2010; Masuti et al. 2016; Freed et al. 2017; Agata et al. 2019). However, extracting constraints on steady-state creep from postseismic deformation is a challenging problem because transient creep is also thought to play an important role (e.g., Pollitz 2003; Freed et al. 2010). The analysis of postseismic deformation is often conducted with the assumption that steady-state creep is well understood (e.g., Freed et al. 2012; Masuti et al. 2016), but as explained in the previous section, most of steady-state flow-law parameters are still poorly constrained by laboratory experiments. Also, the flow law of transient creep itself is still a matter of debate, and existing viscosity estimates from postseismic deformation all depend on the assumed form of mantle rheology, which varies among different studies. Nevertheless, utilizing postseismic deformation is a promising direction given the prospects for the quantity and quality of future data.

Returning to the rheology of oceanic lithosphere, different weakening mechanisms predict different structural consequences, which may be tested against observations. For example, the grain-size reduction hypothesis, when applied to growing oceanic lithosphere, predicts a grain size of 1 μm throughout a mature oceanic lithosphere if stress associated with asthenospheric drag is as high as 50 MPa (Mulyukova and Bercovici 2018). Mantle xenoliths offer the most direct way to observe grain size, but most of mantle xenoliths are from continental lithosphere. Rare mantle xenoliths, derived from $\sim$140-Ma oceanic lithosphere through petit-spot volcanism, exhibit a grain size of $\sim$1 mm (Yamamoto et al. 2014, see Supplementary Information); the absence of grain-size reduction is actually consistent with the stress level expected for the asthenosphere, which is on the order of only 0.1 MPa (Chu and Korenaga 2012). The thermal cracking hypothesis predicts that the oceanic lithosphere is pervasively fractured by a cascade crack system, down to the isotherm of $\sim$700 °C (Korenaga 2007b). In principle, such a structure can be tested by combining lithospheric-scale active-source seismic imaging (e.g., Lizarralde et al. 2004) with high-resolution magnetotelluric imaging. Also, hydration associated with thermal cracking should reduce the "effective" thermal expansivity of oceanic lithosphere (Korenaga 2007a), which seems to be consistent with the seafloor subsidence data (Korenaga and Korenaga 2008, 2016).

The efforts to constrain the rheology of the oceanic upper mantle are thus quite diverse and still in a state of flux. There is also a new inverse approach to estimate flow-law parameters relevant to lithospheric dynamics by running a massive number of regional-scale convection models

(Baumann et al. 2014; Baumann and Kaus 2015). In addition to this, promising directions to explore further include lithospheric flexure by seamount loading, convective instabilities beneath old seafloor or around fracture zones, and postseismic deformation. To properly interpret pertinent observations in terms of mantle rheology, we need to improve our theoretical understanding in each of these areas. For example, to understand the dynamical origin of small-scale mantle density anomalies found beneath fracture zones, it is not sufficient to study how convective instability develops beneath a fracture zone using simple, Newtonian temperature-dependent rheology. This is because the development of convective instability is expected to invoke multiple deformation mechanisms; the incipient growth of instabilities is likely to take place in the diffusion creep regime, but dislocation creep can also be triggered as the instability continues to raise the stress level. The investigation of convective instability with such a composite rheology is yet to be done with a proper understanding of the uncertainties associated with relevant flow-law parameters (section 3.3), even for the simplest case of half-space cooling, let alone the case of horizontally-varying thermal structure expected beneath fracture zones.

3.5 Implementation in numerical simulations

Regarding the implementation of mantle rheology, numerical simulation studies on mantle dynamics may be classified into two categories: (1) those which aim to incorporate as many realistic complications as possible, and (2) those which aim to use the simplest possible form of rheology for a given problem. Perhaps the most familiar example of the first category is those associated with seismic anisotropy (e.g., Kneller et al. 2005; Blackman 2007; Hedjazian et al. 2017). In order to compare with seismological observations, we put in what is known about mineral physics and geodynamics as much as possible, and try to infer flow patterns from observed seismic anisotropy. Dislocation creep responsible for the generation of seismic anisotropy takes place only when deviatoric stress exceeds some critical value, below which diffusion creep predominates, and this critical stress is known to depend on temperature, pressure, grain size, water content, and melt fraction.

Thus, connecting mantle flow and seismic anisotropy requires modeling with composite rheology, which deals with this delicate competition between different creep mechanisms. Clearly, a careful treatment of flow-law uncertainty is required in this type of modeling if one wants to evaluate the reliability of geodynamical predictions. In the second category, on the other hand, we treat mantle rheology as free parameters. One classic example is the scaling law for stagnant lid convection (e.g., Grasset and Parmentier 1998; Dumoulin et al. 1999; Solomatov and Moresi 2000), which quantifies the efficiency of heat transport of thermal convection when viscosity depends strongly on temperature. To address this kind of question, we usually run a series of models by systematically varying rheological parameters such as activation energy and reference viscosity. We then seek a scaling law that can capture the overall behavior of the system under consideration. Because we need to explore the parameter space systematically and extensively, the form of rheology must be simple for this approach to succeed.

These two types of approach can also be seen for the numerical simulation of plate tectonics. Studies of the first type can be quite complex (e.g., Sizova et al. 2010; Gerya et al. 2015), to the extent that the uncertainty of mantle rheology, which is significant on its own (section 3.3), is dwarfed by other possible sources of uncertainty. For models with realistic complications, testing for every source of uncertainty is impractical, and it may not be necessary to begin with if the purpose of modeling is just to provide some stimulating ideas. But when we do decide to investigate the impact of uncertainty on modeling results, the uncertainty under consideration has to be treated properly. Alisic et al. (2012), for example, conducted an impressive set of global plate tectonics simulations with realistic mantle rheology, to investigate the relation between rheology and surface observables, and they found that modeling results are highly sensitive to the stress exponent of dislocation creep. Their exploration of flow-law parameters, however, is inconsistent with how flow-law parameters are constrained by laboratory experiments. They changed the stress exponent independently from other flow-law parameters, and the lack of parameter correlation in their analysis undermines the claimed sensitivity of stress exponent (Mullet et al. 2015).

The second approach, with simplified rheology, is common when investigating the style of mantle convection, e.g., under what conditions plate tectonics can take place. With strongly temperature-dependent viscosity, thermal convection is known to be in the mode of stagnant lid convection (Solomatov 1995), and by adding a weakening mechanism, which usually has simple parameterization, it is possible to escape from the stagnant lid regime. The purpose of this type of research is to understand the dependence of the style of mantle convection on the temperature dependency of viscosity, reference viscosity, and additional parameters that characterize a given weakening mechanism. As this is directly related to one of the questions that this review paper tries to address ("Why does plate tectonics take place on Earth?"), the details of relevant numerical implementations are explained in the following. The strength of the top thermal boundary layer is what matters here, so the key is how to approximate upper-mantle rheology. In this regard, it is important to understand that a certain kind of approximation is meaningful under only some specific contexts. That is, even if some particular approximation is adopted in a well-received study, it does not necessarily mean that the approximation remains appropriate in other situations. The following exposition thus focuses not only on typical numerical implementations of upper-mantle rheology, but also on their footing on rock mechanics as well as their valid range of application.

To capture the strongly temperature-dependent nature of mantle rheology, the following form of viscosity is often used:

$$\eta(T) = \eta_0 \exp\left(\frac{E}{RT} - \frac{E}{RT_0}\right), \tag{12}$$

where η_0 is reference viscosity defined at T_0. This is Newtonian viscosity (i.e., viscosity does not depend on stress) with the Arrhenius form of temperature dependence, corresponding to diffusion creep. Compared with equation (5) or (6), dependence on other than temperature is neglected for simplicity. The lack of grain-size dependence is usually acceptable, because we have little understanding of grain-size variations in the mantle. The omission of pressure dependence is also acceptable because the typical range of activation volume (i.e., on the order of 10 $\mathrm{cm^3\ mol^{-1}}$) does not lead to a substantial viscosity increase in the upper mantle. Given the various uncertainties associated with the eight flow laws for olivine aggregates (equations (3)-(10)), using equation (12) is generally justifiable except, of course, when we want to study the competition between those flow laws, e.g., under what conditions dislocation creep dominates over diffusion creep. Equation (12) may even serve as a rough substitute for non-Newtonian viscosity if the activation energy is scaled down properly with the stress exponent (Christensen 1984).

When the range of temperature variations within the mantle is given by ΔT and the surface temperature is denoted by T_s, the absolute temperature of the mantle varies from T_s to $T_s + \Delta T$. Then, the nondimensional form of equation (12) may be expressed as

$$\eta^*(T^*) = \exp\left(\frac{E^*}{T^* + T_s^*} - \frac{E^*}{1 + T_s^*}\right), \tag{13}$$

where η^* is normalized by reference viscosity defined at $T_s + \Delta T$, E^* is normalized activation energy given by $E/(R\Delta T)$, T^* is normalized temperature varying from 0 to 1, and T_s^* corresponds to $T_s/\Delta T$. Equation (13) may further be approximated as

$$\eta^*(T^*) = \eta_0 \exp[\theta(1 - T^*)], \tag{14}$$

where θ is the Frank-Kamenetskii parameter defined as

$$\theta = \frac{E^*}{(1 + T_s^*)^2} = \frac{E\Delta T}{R(T_s + \Delta T)^2}. \tag{15}$$

This is a linear-exponential approximation of equation (13), having the same temperature dependence as the original Arrhenius form at $T^* = 1$ (Figure 7a).

It is common to weaken temperature-dependent viscosity by combining with nonlinear effective viscosity corresponding to plastic deformation as (Moresi and Solomatov 1998):

$$\eta^* = \left(\frac{1}{\eta^*(T^*)} + \frac{1}{\eta_y^*}\right)^{-1}, \tag{16}$$

where η_y^* is defined as

$$\eta_y^* = \frac{\tau_y^*}{e_{\mathrm{II}}^*}. \tag{17}$$

This is the so-called pseudoplastic rheology. Here τ_y^* is nondimensional yield stress, and e_{II}^* is the second invariant of the nondimensional strain rate tensor. The effective viscosity η_y^* is determined such that stress does not exceed the given yield stress. The use of harmonic mean in equation (16) ensures that the lower of these two viscosities controls the rate of deformation. As may be seen from Figure 5, imposing the yield strength of 100 MPa, which is a common choice in a number of numerical studies with this pseudoplastic viscosity, is equivalent to using the effective viscosity of 10^{23} Pa s with the geological strain rate.

A few examples of purely temperature-dependent viscosity are shown in Figure 7a. The Arrhenius form of temperature dependence is super-exponential, and with the activation energy of 300 kJ mol^{-1}, viscosity changes by $\sim$47 orders of magnitude for the temperature range expected for lithosphere (Figure 7a, solid). Its linear exponential approximation is characterized by the Frank-Kamenetskii parameter of 18.5, and the total viscosity contrast is limited to just eight orders of magnitude (Figure 7a, dashed). The linear exponential approximation is perfectly adequate when modeling stagnant lid convection or small-scale convection, because only the warm part of the lithosphere (with a temperature difference of $\sim$2.4 $\Delta T/\theta$, which is $\sim$175 K in this example; (Solomatov and Moresi 2000)) is mobile enough to participate in convection; the exact strength of the colder part becomes unimportant in such a context. However, when discussing which weakening mechanism is most important for the operation of plate tectonics, simulating realistic temperature-dependent viscosity (i.e., using the Arrhenius form of temperature dependence) becomes important. It would be difficult to test the efficacy of a certain weakening mechanism if the lithosphere to be weaken does not have a realistic strength. Nevertheless, this point tends to be overlooked in numerical studies that attempt to simulate plate tectonics, even when the main goal of study is to discuss conditions for plate tectonics. For example, the convection models of O'Neill and his colleagues (e.g., O'Neill et al. 2007; O'Neill et al. 2016) employ the Frank-Kamenetskii parameter of $\sim$11 (Figure 7a, red). Though such a value is sufficient to simulate stagnant lid convection in the absence of any weakening mechanism, it makes the model lithosphere considerably more sensitive to additional weakening than the real lithosphere; combined with the effective viscosity of 10^{23} Pa s (i.e., the yield strength of 100 MPa), the stiff core of the lithosphere practically vanishes (Figure 7b, red). Another problematic approach is to use the Arrhenius form with a realistic activation energy but with a high surface temperature (e.g., 1000 K) (e.g., Nakagawa and Tackley 2005, 2012) Even if the activation energy is realistically high (e.g., 300 kJ mol^{-1}), the use of high surface temperature makes the temperature dependence of viscosity unrealistically low (Figure 7a,b, blue).

Using this pretended Arrhenius rheology is similar to using too low a value for the Frank-Kamenetskii parameter, and both of these approaches are troublesome in another aspect. The temperature dependence of viscosity dictates the nature of small-scale convection by determining how much of the lithosphere can be delaminated, and the lower the Frank-Kamenetskii parameter is, the greater the amount of delaminated lithosphere becomes. Small-scale convection is important for the onset of subduction (Solomatov 2004). Therefore, using an unrealistically low value for the Frank-Kamenetskii parameter is problematic in two ways: (1) it makes the whole lithosphere so weak that even an ineffective weakening mechanism could appear to be effective, and (2) it makes small-scale convection unrealistically strong, again, helping to validate ineffective weakening mechanisms.

Also, the use of constant yield strength, as shown in Figure 7b, is fairly common in previous studies, but as noted in section 3.1, it is equivalent to assuming a very high cohesive strength with zero friction coefficient. While we may regard this as the depth-averaged brittle strength, the style of mantle convection is sensitive to whether the brittle strength is depth-dependent or not; the so-called intermittent plate tectonics regime appears to require that the yield strength is depth-independent (Moresi and Solomatov 1998). If the strength of lithosphere is reduced by the effect of high pore fluid pressure on friction, as assumed in the thermal cracking hypothesis

(Figure 5d), such a convection regime is unlikely because the brittle strength depends on depth and has a negligible cohesive strength.

Simulating plate tectonics with grain-size reduction has a rock mechanics basis, but as discussed in section 3.2 and shown in Figure 5c, grain-size reduction by itself does not weaken lithosphere sufficiently. Although this seem to conflict with what is suggested by existing numerical studies (e.g., Foley et al. 2014; Foley 2018), there is no real contradiction. We can derive an assumed scaling law for grain size from other scaling laws given in Foley and Bercovici (2014) and Foley et al. (2014), and the grain size required by their theory for the present-day plate tectonics can be shown to be as small as $\sim$50 nm. Also, they exclude the top 20 km of oceanic lithosphere from consideration because brittle deformation is beyond the scope of their theory. Grain-size reduction is expected to play an important role in the operation of plate tectonics, as it allows lithosphere to have the memory of localized weakness and maintain long-lived plate boundaries (e.g., Bercovici and Ricard 2014), but it probably needs to be combined with other weakening mechanisms to make the entire lithosphere deformable.

Rheology is the most important element in mantle dynamics, and given its considerable uncertainty, setting up a meaningful numerical model presents a challenge, if we wish to obtain modeling results that are robust even with rheological uncertainties taken into account. For a model full of realistic complications, we would not be able to test all possible uncertainties. However, if we just want to demonstrate, for example, that the uncertainty of mantle rheology is not important for certain modeling results, it may suffice to conduct a few additional runs in which some end-member mantle rheology (e.g., very high and very low viscosities) is used. For a model with simplified rheology, choosing a proper parameterization for a given problem is of central importance, and it is hoped that a collection of caveats presented in this section will be useful for future modeling studies on the style of mantle convection or the conditions of plate tectonics.

4 Some outstanding questions: A status report

With these preparations, Now I return to the three questions raised in the introduction section.

4.1 Why does plate tectonics take place on Earth?

The question of why plate tectonics takes place on Earth is closely connected to the question of when and how plate tectonics began on Earth, which has also attracted a variety of ideas, such as the spreading of weak continental lithosphere (Rey et al. 2014), the impingement of a plume head (Gerya et al. 2015), and lithospheric damage by bolide impacts (O'Neill et al. 2017). These hypotheses require a particular situation that is only attainable in the early Earth. Also, in these numerical studies, the lithosphere is weakened differently, and it is worth examining whether each of these different implementations can be justified. For example, Rey et al. (2014) used the cohesion strength of 40 MPa and the reference friction coefficient of 0.268, and the friction coefficient is lowered (down to 0.01) as strain accumulated. As noted in section 3.1, compared to laboratory measurements, the cohesion strength is too high, and the friction coefficient is too low unless some additional mechanism is assumed. Also, no justification is given for why the friction coefficient can be reduced to such a low value by mere deformation. Likewise, the efficacy of melt-induced weakening devised by Gerya et al. (2015) depends on the geometry of melt migration through lithosphere, and the formulation of mantle rheology in the simulation of O'Neill et al. (2017) partly inherits the questionable parameterization of O'Neill et al. (2007) (section 3.5). Nevertheless, it is still interesting to ask whether the initiation of plate tectonics was made possible by some mechanisms that could happen only in the early Earth and whether such an initiation is also responsible for the subsequent operation of plate tectonics to the present. They are unresolved questions.

If we take a less history-dependent view, i.e., the long-term operation of plate tectonics is enabled by the persistence of certain conditions, then, the lithosphere needs to be weaken by some mechanisms that can take place even at present. Such mechanisms have better chances to be investigated by various angles, and our understanding of the strength of present-day oceanic lithosphere (section 3.2) becomes important. As the influence of grain-size reduction is likely to be limited to the relatively warm part of lithosphere, we need to identify a weakening mechanism for the cold part, or more specifically, a 'physical' mechanism that can reduce the effective friction coefficient. For example, the aforementioned strain-dependent friction coefficient used by Rey et al. (2014) could potentially be related to the gradual maturation of faults with large-scale deformation. In the field of earthquake dynamics, a variety of mechanisms have been suggested to reduce friction during fault slip, including flash heating and thermal pressurization (e.g., Rice 2006), and as faults grow, greater fault slips become possible, activating more dynamic weakening mechanisms that require large enough slip or large enough rise in fault temperature (Di Toro et al. 2004; Rempel and Rice 2006; Han et al. 2007). It remains to be seen whether a strain-dependent friction coefficient emerges from the coarse-graining of a system with evolving faults.

Thermal cracking can also be such a physical mechanism. One interesting aspect of this mechanism is that it turns the rheological predicament to good advantage; the strongly temperature-dependent viscosity of silicate rocks facilitates thermal cracking, because higher viscosity leads to higher thermal stress (e.g., Boley and Weiner 1960; Muki and Sternberg 1961). Note that creating tension cracks by itself does not reduce the friction coefficient and thus the yield strength. To reduce the friction coefficient over an order of magnitude, as assumed in Figure 5d, the surface openings of cracks have to be closed by serpentinization to trap water within the cracks; high fluid pressure in such trapped water, likely achieved under tectonic compression, can then reduce the effective friction coefficient, in principle, down to almost zero. This process do not take place in the absence of surface water, so the thermal cracking hypothesis for the onset of plate tectonics naturally explains why plate tectonics is not observed on Venus and Mars. Venus is simply too close to the Sun to maintain surface water (Hamano et al. 2013), and Mars is too small to do so on a geological time scale (e.g., Shizgal and Arkos 1996). The contrasting tectonic styles on Earth and Venus have motivated other explanations based on high surface temperatures on Venus (e.g., Lenardic et al. 2008; Landuyt and Bercovici 2009; Karato and Barbot 2018), but such explanations do not address the lack of plate tectonics on Mars.

However, the thermal cracking hypothesis is not fully expounded yet, and it requires further theoretical and observational efforts. The numerical modeling of Korenaga (2007b) is limited to single-crack systems, and the coevolution of serpentinization and crack growth, as speculated by Korenaga (2017a), needs to be modeled quantitatively. The most prominent manifestation of thermal cracking is transform faults and fracture zones (Turcotte and Oxburgh 1973; Turcotte 1974). The spacing of such features is too large to release all of thermal stress expected from the cooling of oceanic lithosphere, but smaller-scale crack systems have not been directly observed. So far, the state of pervasively cracked oceanic lithosphere is inferred only indirectly, based on the seismic structure of shallow oceanic lithosphere (Lizarralde et al. 2004; Korenaga 2007b), reduced effective thermal expansivity (Korenaga and Korenaga 2008, 2016), and the spatial distribution of lower-plane earthquakes in the double seismic zone (Kita et al. 2010; Korenaga 2017a). There is also a possibility to test the prediction of horizontal thermal contraction, which is directly related to thermal stress, with future space geodetic data (Kreemer and Gordon 2014).

4.2 Can we predict surface topography from first principles?

The surface of Earth is varied with continents and ocean basins, and it would be impractical to theoretically predict such complex features, many details of which have been shaped by historical accidentals. Characterizing the statistical nature of large-scale surface topography may be less prohibitive, but even if we limit ourselves to ocean basins, the task is far from being trivial.

The most straightforward part is the normal seafloor unaffected by the emplacement of hotspot islands and oceanic plateaus, because its topography is mostly controlled by subsidence after its creation at mid-ocean ridges. To characterize the overall topography of such a normal part of seafloor, however, we need to know plate velocity as well as the size distribution of oceanic plates. It is possible to predict average plate velocity from mantle potential temperature (e.g., Christensen 1985; Korenaga 2010), but a scaling law for plate size distribution is not yet available. The current lack of such a scaling law is understandable because the size distribution, i.e., the planform of mantle convection with plate tectonics, is expected to depend on the weakening mechanism of oceanic lithosphere. Based on the subductability of oceanic lithosphere, the size distribution is estimated to have been largely constant at least back to $\sim$3 Ga (Korenaga 2006), but this is merely an empirical constraint. Furthermore, the details of seafloor subsidence depends not only on the material properties that affect thermal contraction, i.e., thermal expansivity, thermal conductivity, specific heat, and density (Turcotte and Oxburgh 1967; Davis and Lister 1974), and those that control small-scale convection such as temperature- and depth-dependent viscosity (Davaille and Jaupart 1994; Korenaga and Jordan 2002b), but also on thermal cracking, radiogenic heat production, and the secular cooling of Earth (Korenaga and Korenaga 2016).

The emplacement of hotspot islands and oceanic plateaus can disturb significantly the otherwise steady seafloor subsidence. The fraction of seafloor characterized with thick igneous crust resulting from such anomalous magmatism is only $\sim$10 %, but the fraction of seafloor affected by the emplacement of such anomalous crust (e.g., by the spreading of plume materials beneath lithosphere) is much greater ($>$ 50 %) (see Figure 7 of Korenaga and Korenaga (2008)). Predicting the magnitude of such anomalous magmatism and its frequency, from a purely theoretical ground, is difficult. Even if we assume that all of such anomalous magmatism originates from mantle plumes, predicting the plume flux from the core heat flux is not easy (Labrosse 2002; Zhong 2006), especially given the uncertainty associated with the rheology of the lower mantle (Solomatov 1996; Korenaga 2005a). The magnitude of present-day core heat flux is quite uncertain to begin with (e.g., Lay et al. 2008), and predicting the evolution of core heat flux requires modeling of the thermal evolution of the entire Earth (e.g., Stevenson et al. 1983; O'Rourke et al. 2017).

More important, it is unlikely that mantle plumes are responsible for all of such anomalous magmatism (e.g., Anderson 1995; Foulger et al. 2005). The inevitable existence of chemical heterogeneities, as introduced by the operation of plate tectonics (section 2.4), could account for the formation of at least some oceanic plateaus, including Ontong Java Plateau (Korenaga

2005b, 2011b) and Shatsky Rise (Korenaga and Sager 2012). The degree of chemical heterogeneities in the convecting mantle is still poorly constrained. A number of geochemical as well as seismological studies indicate that the mantle is chemically heterogeneous at a range of scales (e.g., Zindler and Hart 1986; Gudmundsson et al. 1990; Hofmann 1997; Kaneshima and Helffrich 1998; Korenaga and Kelemen 2000; Margerin and Nolet 2003; Trampert et al. 2004; Sobolev et al. 2007; Korenaga 2015a), but understanding the origin of such inferred heterogeneities and their relation to plate tectonics requires us to better understand the efficiency of convecting mixing, which depends on mantle rheology.

4.3 How does plate tectonics control surface environment?

Plate tectonics of course affects, either directly or indirectly, most of surface environment, from the generation of continental crust (Campbell and Taylor 1983) to the modulation of atmospheric composition (Berner 2004). Here I focus on the role of the oceanic upper mantle in the relation between plate tectonics and surface environment. Perhaps the most important is its influence on global sea level change, which controls the spatial extent of dry landmasses, which in turn controls various geochemical cycles as well as the planetary albedo. Even with abundant continental crust, the existence of dry landmasses is not guaranteed; too shallow ocean basins or too much ocean water can inundate continents. Both seafloor topography and ocean volume can vary with time, and both are influenced by the evolution of the oceanic upper mantle.

Global sea level or, equivalently, the continental freeboard (the relative height of mean continental landmasses with respect to the sea level) is controlled by a number of components, including continental crust, continental mantle lithosphere, oceanic crust, depleted oceanic mantle lithosphere, asthenospheric mantle, and ocean volume, all of which exhibit secular evolution (Korenaga et al. 2017). It is important to understand the complexity of the problem. The growth of continental crust is more or less a geochemical problem (e.g., Armstrong 1981; Jacobsen 1988; Campbell 2003; Korenaga 2018), but the emergence of continental crust above the sea level involves both geophysics and geochemistry. The first-order control on the continental freeboard is brought by the relative buoyancy of the continental lithosphere with respect to the oceanic lithosphere. The intrinsic density structure of oceanic lithosphere is determined by mantle melting at mid-ocean ridges, which is a function of mantle potential temperature (McKenzie and Bickle 1988; Langmuir et al. 1992). That of continental lithosphere is also likely governed by mantle potential temperature (Kelemen et al. 1998; Herzberg 2004; Servali and Korenaga 2018), though the density of continental lithosphere at any given time is not a simple function of potential temperature because the structure of continental lithosphere reflects the history of lithospheric formation over the last three billion years. The zero-age depth of seafloor is controlled by this relative buoyancy between continental and oceanic lithosphere, and the capacity of ocean basins is determined by the zero-age depth as well as the subsequent evolution of seafloor topography. As summarized in the previous section, seafloor subsidence is affected by quite a few factors, and a new kind of physics-based reference model discussed in section 2.5 would become invaluable in this context.

The volume of oceans can vary with time, depending on a dynamic balance between water gain by mantle degassing and water loss by subduction. The present-day global water budget has consistently pointed to positive net water influx into the mantle (Ito et al. 1983; Jarrard 2003) (note that a zero influx estimate by Parai and Mukhopadhyay (2012) is based on their assumption of time-invariant hypsometry), and continental freeboard modeling also suggests long-term net water influx of 3-4.5 $\times 10^{14}$ g yr^{-1} over the last three billion years (Korenaga et al. 2017). Thus, the oceans are likely to have been more voluminous in the past, and correspondingly, the convecting mantle must have been drier. As predicted by freeboard modeling (Korenaga et al. 2017) and also suggested by geological and geochemical data (Arndt 1999; Bindeman et al. 2018; Johnson and Wing 2020), the early Archean is likely to have been a ‘water world’ with little stable dry landmass, and the gradual subduction of water, made possible by the seawater alteration of oceanic lithosphere, is essential to bring continents above the sea level. At the same time, the concurrent hydration of the convecting mantle results in the relative strengthening of continental lithospheric mantle (Korenaga

2013), which affects the efficiency of crustal recycling through time (Rosas and Korenaga 2018; Guo and Korenaga 2020). Thus, the seawater alteration of oceanic lithosphere, which by itself a very shallow process, has far-reaching effects on the coevolution of Earth's interior and surface environment over billions of years.

5 Future directions

I have already pointed out, at various places in this paper, what is critically needed to improve our understanding of the oceanic upper mantle and its role in the big picture of Earth evolution. Our to-do list includes the degree of hydration of oceanic lithosphere, the nature of chemical heterogeneities in the mantle, the role of small-scale convection in the lithosphere-asthenosphere boundary, a new kind of physics-based reference model, and better experimental and observational constraints on mantle rheology. Most of these issues are under active research. Here I would like to conclude with two overarching statements.

The operation of plate tectonics is widely believed to be essential to build an Earth-like planet, so conditions for plate tectonics have important implications for the origins of life in the universe at large. Without the subduction of oceanic plates, plate tectonics is impossible to take place, and a better understanding of oceanic lithosphere must come from marine geophysics. Thus, future observational efforts in the field of marine geophysics, if they are targeted toward the nature of normal oceanic lithosphere, could achieve lasting impacts on the broad community of earth and planetary sciences, just as marine geophysics played a pivotal role in the plate tectonics revolution in the 1960s and 1970s. For example, a more direct observational test of the thermal cracking hypothesis may be possible by combining active-source seismology and magnetotelluric imaging. For such an effort to be successful, the hypothesis also needs to be theoretically refined to yield more detailed predictions to be compared with observations.

However uncertain at the moment, mantle rheology is the most important factor in geodynamics, and given its complex functionality, numerical modeling is essential. When designing a numerical model, a variety of approximations are possible and often necessary, and when doing so, it is always worthwhile to honor the current uncertainties of rock mechanics. It is better to test at least a few candidate rheological models, to represent the existing uncertainties or to demonstrate model sensitivity to mantle rheology. As earth and planetary sciences progress, various branches have gradually been compartmentalized, to the extent that most of non-geodynamicists cannot critically evaluate modeling studies. The well-being of geodynamics thus hinges on how the current generation of geodynamicists discipline themselves, digest rock mechanics, and strive to construct meaningful models. Otherwise, modeling results may soon (if not already) be seen arbitrary, carrying little scientific weight.

Competing interests

The authors declare that they have no competing interest.

Funding

This work was supported in part by U.S. National Science Foundation OCE-1736563 and the U.S. National Aeronautics and Space Administration through the NASA Astrobiology Institute under Cooperative Agreement No. NNA15BB03A issued through the Science Mission Directorate.

Availability of Data and Materials

This work is a review of the existing relevant literature, and there is no additional data.

Acknowledgments

The author thanks Shun-ichiro Karato for discussion on mantle rheology. The author also thanks Hitoshi Kawakatsu for his constructive comments on the earlier version of the manuscript and two official reviewers, Norm Sleep and Taras Gerya, for a number of helpful comments and suggestions.

References

Agata, R., Barbot, S. D., Fujita, K., Kyodo, M., Iinuma, T., Nakata, R., Ichimura, T., Hori, T., 2019. Rapid mantle flow with power-law creep explains deformation after the 2011 Tohoku mega-quake. Nature Comm. 10, 1385, https://doi.org/10.1038/s41467–019–08984–7.

Aharonov, E., Scholz, C. H., 2019. The brittle-ducitle transition predicted by a physics-based friction law. J. Geophys. Res. Solid Earth 124, https://doi.org/10.1029/2018JB016878.

Alisic, L., Gurnis, M., Stadler, G., Burstedde, C., Ghattas, O., 2012. Multi-scale dynamics and rheology of mantle flow with plates. J. Geophys. Res. 117, B10402, doi:10.1029/2012JB009234.

Alt, J. C., Honnorez, J., Laverne, C., Emmermann, R., 1986. Hydrothermal alteration of a 1 km section through the upper oceanic crust, DSDP Hole 504B: The mineralogy, chemistry, and evolution of seawater-basalt interactions. J. Geophys. Res. 91, 10309–10335.

Alt, J. C., Teagle, D. A. H., 2000. Hydrothermal alteration and fluid fluxes in ophiolites and oceanic crust. In: Dilek, Y., Moores, E. M., Elthon, D., Nicolas, A. (Eds.), Ophiolites and Oceanic Crust: New Insights from Field Studies and the Ocean Drilling Program. Vol. 349 of Geol. Soc. Am. Special Paper. Geol. Soc. Am., Boulder, CO, pp. 273–282.

Anderson, D. L., 1995. Lithosphere, asthenosphere, and perisphere. Rev. Geophys. 33, 125–149.

Anderson, D. L., Sammis, C., 1970. Partial melting in the upper mantle. Phys. Earth Planet. Inter. 3, 41–50.

Armstrong, R. L., 1981. Radiogenic isotopes: the case for crustal recycling on a near-steady-state no-continental-growth Earth. Phil. Trans. R. Soc. Lond. A 301, 443–472.

Arndt, N., 1999. Why was flood volcanism on submerged continental platforms so common in the Precambrian? Precambrian Res. 97, 155–164.

Baba, K., Noriko, N., Matsuno, T., Liang, P., Li, R., Zhang, L., Shimizu, H., Abe, N., Hirano, N., Ichiki, M., Utada, H., 2017. Electrical conductivity of old oceanic mantle in the northwestern Pacific, I, 1-D profiles suggesting differences in thermal structure not predictable from a plate cooling model. Earth Planets Space 69, 111, doi:10.1186/s40623–017–0697–0.

Bai, Q., Mackwell, S. J., Kohlstedt, D. L., 1991. High-temperature creep of olivine single crystals, 1, mechanical results for buffered samples. J. Geophys. Res. 96, 2441–2463.

Ballmer, M. D., van Hunen, J., Ito, G., Tackley, P. J., Bianco, T. A., 2007. Non-hotspot volcano chains originating from small-scale sublithospheric convection. Geophys. Res. Lett. 34, L23310, doi:10.1029/2007GL031636.

Baumann, T. S., Kau, B. J. P., Popov, A. A., 2014. Constraining effective rheology through parallel joint geodynamic inversion. Tectonophysics 631, 197–211.

Baumann, T. S., Kaus, B. J. P., 2015. Geodynamic inversion to constrain the non-linear rheology of the lithosphere. Geophys. J. Int. 202, 1289–1316.

Behn, M. D., Kelemen, P. B., 2003. Relationship between seismic P-wave velocity and the composition of anhydrous igneous and meta-igneous rocks. Geochem. Geophys. Geosys. 4, 1041, doi:10.1029/2002GC00393.

Bercovici, D., Ricard, Y., 2012. Mechanisms for the generation of plate tectonics by two-phase grain-damage and pinning. Phys. Earth Planet. Inter. 202-203 (27-55).

Bercovici, D., Ricard, Y., 2014. Plate tectonics, damage and inheritance. Nature 508, 513–516.

Bercovici, D., Skemer, P., 2017. Grain damage, phase mixing and plate-boundary formation. J. Geodyn. 108, 40–55.

Bercovici, D., Tackley, P. J., Ricard, Y., 2015. The generation of plate tectonics from mantle dynamics. In: Treatise on Geophysics, 2nd ed. Vol. 7. Elsevier, pp. 271–318.

Berner, R. A., 2004. The Phanerozoic Carbon Cycle: CO_2 and O_2. Oxford Univ. Press.

Bickle, M. J., Teagle, D. A. H., 1992. Strontium alteration in the Troodos ophiolite: Implications for fluid fluxes and geochemical transport in mid-ocean ridge hydrothrmal systems. Earth Planet. Sci. Lett. 113, 219–237.

Bindeman, I. N., Zakharov, D. O., Palandri, J., Greber, N. D., Dauphas, N., Retallack, G. J., Hofmann, A., Lackey, J. S., Bekker, A., 2018. Rapid emergence of subaerial landmasses and onset of a modern hydrologic cycle 2.5 billion years ago. Nature 557, 545–548.

Blackman, D. K., 2007. Use of mineral physics, with geodynamic modelling and seismology, to investigate flow in the Earth's mantle. Rep. Prog. Phys. 70, 659–689.

Boley, B. A., Weiner, J. H., 1960. Theory of Thermal Stresses. John Wiley & Sons, New York.

Braun, J., Chery, J., Poliakov, A., Mainprice, D., Vauchez, A., Tomassi, A., Daignieres, M., 1999. A simple parameterization of strain localization in the ductile regime due to grain size reduction: A case study for olivine. J. Geophys. Res. 104, 25167–25181.

Buck, W. R., Lavier, L. L., Poliakov, A. N. B., 2005. Modes of faulting at mid-ocean ridges. Nature 434, 719–723.

Buck, W. R., Parmentier, E. M., 1986. Convection beneath young oceanic lithosphere: Implications for thermal structure and gravity. J. Geophys. Res. 91, 1961–1974.

Byerlee, J., 1978. Friction of rocks. PAGEOPH 116, 615–626.

Cadio, C., Korenaga, J., 2012. Localization of geoid anomalies and the evolution of oceanic lithosphere: A case study from the Mendocino Fracture Zone. J. Geophys. Res. 117, B10404, doi:10.1029/2012JB009524.

Cadio, C., Korenaga, J., 2014. Resolving the fine-scale density structure of shallow oceanic mantle by Bayesian inversion of locaized geoid anomlaies. J. Geophys. Res. Solid Earth 119, 3627–3645, doi:10.1002/2013JB010840.

Cadio, C., Korenaga, J., 2016. Macroscopic strength of oceanic lithosphere revealed by ubiquitous fracture-zone instabilities. Earth Planet. Sci. Lett. 449, 295–301.

Cai, C., Wiens, D. A., Shen, W., Eimer, M., 2018. Water input into the Mariana subduction zone estimated from ocean-bottom seismic data. Nature 563, 389–392.

Campbell, I. H., 2003. Constraints on continental growth models from Nb/U ratios in the 3.5 Ga Barberton and other Archaean basalt-komatiite suites. Am. J. Sci. 303, 319–351.

Campbell, I. H., Taylor, S. R., 1983. No water, no granites - no oceans, no continents. Geophys. Res. Lett. 10, 1061–1064.

Canales, J. P., Carbotte, S. M., Nedimovic, M. R., Carton, H., 2017. Dry Juan de Fuca slab revealed by quantification of water entering Cascadia subduction zone. Nature Geosci. 10, 864–870.

Caress, D. W., McNutt, M. K., Detrick, R. S., Mutter, J. C., 1995. Seismic imaging of hotspot-related crustal underplating beneath the Marquises Islands. Nature 373, 600–603.

Carlson, R. L., 2003. Bound water content of the lower oceanic crust estimated from modal analyses and seismic velocities of oceanic diabase and gabbro. Geophys. Res. Lett. 30, 2142, doi:10.1029/2003GL018213.

Carlson, R. L., Johnson, H. P., 1994. On modeling the thermal evolution of the oceanic upper mantle: An assessment of the cooling model. J. Geophys. Res. 99, 3201–3214.

Carlson, R. L., Miller, D. J., 2004. Influence of pressure and mineralogy on seismic velocities in oceanic gabbros: Implications for the composition and state of the lower oceanic crust. J. Geophys. Res. 109, B09205, doi:10.1029/2003JB002699.

Carmody, L., Barry, P. H., Shervais, J. W., Kluesner, J. W., Taylor, L. A., 2013. Oxygen isotopes in subducted oceanic crust: A new perspective from Siberian diamondiferous eclogites. Geochem. Geophys. Geosys. 14, 3479–3493, doi:10.1002/ggge.20220.

Chantel, J., Manthilake, G., Andrault, D., Novella, D., Yu, T., Wang, Y., 2016. Experimental evidence supports mantle partial melting in the asthenosphere. Sci. Adv. 2, 31600246, doi:10.1126/sciadv.1600246.

Chester, F. M., 1995. A rheologic model for wet crust applied to strike-slip faults. J. Geophys. Res. 100 (B7), 13033–13044.

Chopra, P. N., Paterson, M. S., 1984. The role of water in the deformation of dunite. J. Geophys. Res. 89, 7861–7876.

Christensen, N. I., 2004. Serpentinites, peridotites, and seismology. Int. Geol. Rev. 46, 795–816.

Christensen, N. I., Smewing, J. D., 1981. Geology and seismic structure of the northern section of the Oman ophiolite. J. Geophys. Res. 86, 2545–2555.

Christensen, U., 1984. Convection with pressure- and temperature-dependent non-Newtonian rheology. Geophys. J. R. Astron. Soc. 77, 343–384.

Christensen, U. R., 1985. Thermal evolution models for the Earth. J. Geophys. Res. 90, 2995–3007.

Chu, X., Korenaga, J., 2012. Olivine rheology, shear stress, and grain growth in the lithospheric mantle: Geological constraints from the Kaapvaal craton. Earth Planet. Sci. Lett. 333-334, 52–62.

Cline, C. J., Faul, U. H., David, E. C., Berry, A., Jackson, I., 2018. Redox-influenced seismic properties of upper-mantle olivine. Nature 555, 355–358.

Coffin, M. F., Eldholm, O., 1994. Large igneous provinces: Crustal structure, dimensions, and external consequences. Rev. Geophys. 32, 1–36.

Coffin, M. F., Gahagan, L. M., 1995. Ontong Java and Kerguelen Plateaux: Cretaceous Icelands? J. Geol. Soc London 152, 1047–1052.

Contreras-Reyes, E., Grevemeyer, I., Flueh, E. R., Scherwath, M., Bialas, J., 2008. Effect of trench-outer rise bending-related faulting on seismic Poisson's ratio and mantle anisotropy: a case study offshore of Southern Central Chile. Geophys. J. Int. 173, 142–156.

Courtillot, V., Davaille, A., Besse, J., Stock, J., 2003. Three distinct types of hotspots in the Earth's mantle. Earth Planet. Sci. Lett. 205, 295–308.

Courtney, R. C., Beaumont, C., 1983. Thermally-activated creep and flexure of the oceanic lithosphere. Nature 305, 201–204.

Crosby, A. G., McKenzie, D., Sclater, J. G., 2006. The relationship between depth, age and gravity in the oceans. Geophys. J. Int. 166, 443–573.

Cross, A. J., Skemer, P., 2017. Ultramylonite generation via phase mixing in high-strain experiments. J. Geophys. Res. Solid Earth 122, 1744–1759, doi:10.1002/2016JB013801.

Davaille, A., Jaupart, C., 1994. Onset of thermal convection in fluids with temperature-dependent viscosity: Application to the oceanic mantle. J. Geophys. Res. 99, 19853–19866.

Davies, G. F., 1988. Ocean bathymetry and mantle convection: 1. large-scale flow and hotspots. J. Geophys. Res. 93, 10467–10480.

Davis, E. E., Lister, C. R. B., 1974. Fundamentals of ridge crest topography. Earth Planet. Sci. Lett. 21, 405–413.

Debayle, E., Ricard, Y., 2012. A global shear wave velocity model of the upper mantle from fundamental and higher Rayleigh mode measurements. J. Geophys. Res. 117, B10308, doi:10.1029/2012JB009288.

DeLaughter, J., Stein, S., Stein, C. A., 1999. Extraction of a lithospheric cooling signal from oceanwide geoid data. Earth Planet. Sci. Lett. 174, 173–181.

deMartin, B., Hirth, G., Evans, B., 2004. Experimental constraints on thermal cracking of peridotite at oceanic spreading centers. In: Lin, J. (Ed.), The Thermal Structure of the Oceanic Crust and Dynamics of Hydrothermal Circulation. Vol. 148. American Geophysical Union, Washington, D.C., pp. 167–185.

Di Toro, G., Goldsby, D. L., Tullis, T. E., 2004. Friction falls toward zero in quartz rock as slip velocity approaches seismic rates. Nature 427, 436–439.

Dick, H. J. B., Natland, J. H., Alt, J. C., Back, W., Bideau, D., Gee, J. S., Haggas, S., Hertogen, J. G. H., Hirth, G., Holm, P. H., Ildefonse, B., Iturrino, G. J., John, B. E., Kelley, D. S., Kikawa, E., Kingdon, A., LeRoux, P. J., Maeda, J., Meyer, P. S., Miller, D. J., Naslund, H. R., Niu, Y.-L., Robinson, P. T., Snow, J., Stephen, R. A., Trimby, P. W., Worm, H.-U., Yoshinobu, A., 2000. A long in situ section of the lower ocean crust: results of ODP Leg 176 drilling at the Southwest Indian Ridge. Earth Planet. Sci. Lett. 179, 31–51.

Doin, M.-P., Fleitout, L., Christensen, U., 1997. Mantle convection and stability of depleted and undepleted continental lithosphere. J. Geophys. Res. 102, 2772–2787.

Druiventak, A., Trepmann, C. A., Renner, J., Hanke, K., 2011. Low-temperature plasticity of olivine during high stress deformation of peridotite at lithospheric conditions — an experimental study. Earth Planet. Sci. Lett. 311, 199–211.

Drury, M. R., Vissers, R. L. M., Van der Wal, D., Hoogerduijn Strating, E. H., 1991. Shear localisation in upper mantle pridotites. PAGEOPH 137, 439–460.

Dumoulin, C., Doin, M.-P., Fleitout, L., 1999. Heat transport in stagnant lid convection with temperature- and pressure-dependent Newtonian or non-Newtonian rheology. J. Geophys. Res. 104, 12759–12777.

Dumoulin, C., Doin, M.-P., Fleitout, L., 2001. Numerical simulations of the cooling of an oceanic lithosphere above a convective mantle. Phys. Earth Planet. Inter. 125, 45–64.

Durham, W. B., Mei, S., Kohlstedt, D. L., Wang, L., Dixon, N. A., 2009. New measurements of activation volume in olivine under anhydrous conditions. Phys. Earth Planet. Inter. 172, 67–73.

Dymkova, D., Gerya, T., 2013. Porous fluid flow enables oceanic subduction initiation on Earth. Geophys. Res. Lett. 40, 5671–5676, doi:10.1002/2013GL057798.

Faccenda, M., Gerya, T. V., Burlini, L., 2009. Deep slab hydration induced by bending-related variations in tectonic pressure. Nature Geosci. 2, 790–793.

Faul, U. H., Jackson, I., 2007. Diffusion creep of dry, melt-free olivine. J. Geophys. Res. 112, B04204, doi:10.1029/2006JB004586.

Ferrachat, S., Ricard, Y., 1998. Regular vs. chaotic mantle mixing. Earth Planet. Sci. Lett. 155, 75–86.

Foley, B. J., 2018. The dependence of planetary tectonics on mantle thermal state: applications to early Earth evolution. Phil. Trans. R. Soc. A 376, 20170409, http://dx.doi.org/10.1098/rsta.2017.0409.

Foley, B. J., Bercovici, D., 2014. Scaling laws for convection with temperature-dependent viscosity and grain-damage. Geophys. J. Int. 199, 580–603.

Foley, B. J., Bercovici, D., Elkins-Tanton, L. T., 2014. Initiation of plate tectonics from post-magma ocean thermochemical convection. J. Geophys. Res. Solid Earth 119, 8538–8561, doi:10.1002/2014JB011121.

Forsyth, D., Uyeda, S., 1975. On the relative importance of the driving forces of plate motion. Geophys. J. R. Astron. Soc. 43, 163–200.

Foulger, G. R., Natland, J. H., Presnell, D. C., Anderson, D. L., 2005. Plates, Plumes, and Paradigms. Geological Society of America.

Freed, A. M., Hashima, A., Becker, T. W., Okaya, D. A., Sato, H., Hatanaka, Y., 2017. Resolving depth-dependent subduction zone viscosity and afterslip from postseismic displacements following the 2011 Tohoku-oki, Japan earthquake. Earth Planet. Sci. Lett. 459, 279–290.

Freed, A. M., Herring, T., Bürgmann, R., 2010. Steady-state laboratory flow laws alone fail to explain postseismic observations. Earth Planet. Sci. Lett. 300, 1–10.

Freed, A. M., Hirth, G., Behn, M. D., 2012. Using short-term postseismic displacements to infer the ambient deformation conditions of the upper mantle. J. Geophys. Res. 117, B01409, doi:10.1029/2011JB008562.

Frost, H. J., Ashby, M. F., 1982. Deformation-mechanism maps: The plasticity and creep of metals and ceramics. Pergamon, New York.

Gale, A., Langmuir, C. H., Dalton, C. A., 2014. The global systematics of ocean ridge basalts and their origin. J. Petrol. 55, 1051–1082.

Gans, K. D., Wilson, D. S., Macdonald, K. C., 2003. Pacific plate gravity lineaments: Diffuse extension or thermal contraction? Geochem. Geophys. Geosys. 4 (9), 1074, doi:10.1029/2002GC000465.

Gerya, T. V., Stern, R. J., Baes, M., Sobolev, S. V., Whattam, S. A., 2015. Plate tectonics on the Earth triggered by plume-induced subduction initiation. Nature 527, 221–225.

Gillis, K. M., 1995. Controls on hydrothermal alteration in a section of fast-spreading oceanic crust. Earth Planet. Sci. Lett. 134, 473–489.

Goetze, C., 1978. The mechanisms of creep in olivine. Phil. Trans. R. Soc. Lond. A 288, 99–119.

Goetze, C., Evans, B., 1979. Stress and temperature in the bending lithosphere as constrained by experimental rock mechanics. Geophys. J. R. Astron. Soc. 59, 463–478.

Goutorbe, B., Hillier, J. K., 2013. An integration to optimally constrain the thermal structure of oceanic lithosphere. J. Geophys. Res. 118, 432–446, doi:10.1029/2012JB009527.

Grasset, O., Parmentier, E., 1998. Thermal convection in a volumetrically heated, infinite Prandtl number fluid with strongly temperature-dependent viscosity: Implications for planetary thermal evolution,. J. Geophys. Res. 103, 18171–18181.

Gregory, R. T., Taylor, H. P., 1981. An oxygen isotope profile in a section of Cretaceous oceanic crust, Samail ophiolite, Oman: Evidence for δ^{18}O buffering of the oceans by deep (>5 km) seawater-hydrothermal circulation at mid-ocean ridges. J. Geophys. Res. 86, 2737–2755.

Grevemeyer, I., Ranero, C. R., Ivandic, M., 2018. Structure of oceanic crust and serpentinization at subduction trenches. Geosphere 14, 395–418, doi:10.1130/GES01537.1.

Gudmundsson, O., Davies, J. H., Clayton, R. W., 1990. Stochastic analysis of global traveltime data: mantle heterogeneity and random errors in the ISC data. Geophys. J. Int. 102, 25–43.

Guo, M., Korenaga, J., 2020. Argon constraints on the early growth of felstic continental crust. Sci. Adv. in press.

Hager, B. H., 1983. Global isostatic geoid anomalies for plate and boundary layer models of the lithosphere. Earth Planet. Sci. Lett. 63, 97–109.

Hager, B. H., 1991. Mantle viscosity: A comparison of models from postglacial rebound and from the geoid, plate driving forces, and advected heat flux. In: Sabadini, R., Lambeck, K., Boschi, E. (Eds.), Glacial Isostasy, Sea-Level and Mantle Rheology. Kluwer Academic, Dordrecht, pp. 493–513.

Hamano, K., Abe, Y., Genda, H., 2013. Emergence of two types of terrestrial planet on solidification of magma ocean. Nature 497, 607–610.

Han, R., Shimamoto, T., Hirose, T., Ree, J.-H., Ando, J., 2007. Ultralow friction of carbonate faults caused by thermal decomposition. Science 316, 878–881.

Hansen, L. N., Kumamoto, K. M., Thom, C. A., Wallis, D., Durham, W. B., Goldsby, D. L., Breithaupt, T., Meyers, C. D., Kohlstedt, D. L., 2019. Low-temperature plasticity in olivine: Grain size, strain hardening, and the strength of the lithosphere. J. Geophys. Res. Solid Earth, doi:10.1029/2018JB016736.

Hansen, L. N., Zimmerman, M. E., Kohlstedt, D. L., 2011. Grain boundary sliding in San Carlos olivine: Flow law parameters and crystallographic-preferred orientation. J. Geophys. Res. 116, B08201, doi:10.1029/2011JB008220.

Harmon, N., Forsyth, D. W., Weeraratne, D. S., Yang, Y., Webb, S. C., 2011. Mantle heterogeneity and off axis volcanism on young Pacific lithosphere. Earth Planet. Sci. Lett. 311, 306–315.

Hatakeyama, K., Katayama, I., Hirauchi, K., Michibayashi, K., 2017. Mantle hydration along outer-rise faults inferred from serpentinite permeability. Sci. Rep. 7, 13870, doi:10.1038/s41598–017–14309–9.

Hauri, E. H., 1996. Major-element variability in the Hawaiian mantle plume. Nature 382, 415–419.

Haxby, W. F., Weissel, J. K., 1986. Evidence for small-scale mantle convection from Seasat altimeter data. J. Geophys. Res. 91, 3507–3520.

Hedjazian, N., Garel, F., Davies, D. R., Kaminski, E., 2017. Age-independent seismic anisotropy under oceanic plates explained by strain history in the asthenosphere. Earth Planet. Sci. Lett. 460, 135–142.

Heestand, R. L., Crough, S. T., 1981. The effect of hot spots on the oceanic age-depth relation. J. Geophys. Res. 86, 6107–6114.

Herzberg, C., 2004. Geodynamic information in peridotite petrology. J. Petrol. 45, 2507–2530.

Herzberg, C., Asimow, P. D., Arndt, N., Niu, Y., Lesher, C. M., Fitton, J. G., Cheadle, M. J., Saunders, A. D., 2007. Temperatures in ambient mantle and plumes: Constraints from basalts, picrites, and komatiites. Geochem. Geophys. Geosys. 8 (2), Q02206, doi:10.1029/2006GC001390.

Hillier, J. K., Watts, A. B., 2005. Relationship between depth and age in the North Pacific ocean. J. Geophys. Res. 110, B02405, doi:10.1029/2004JB003406.

Hirano, N., Koppers, A. A. P., Takahashi, A., Fujiwara, T., Nakanishi, M., 2008. Seamounts, knolls and petit-spot monogenetic volcanoes on the subducting Pacific Plate. Basin Res. 20 (543-553, doi:10.1111/j.1365-2117.2008.00363.x).

Hirano, N., Machida, S., Abe, N., Morishita, T., Tamura, A., Arai, S., 2013. Petit-spot lava fields off the central Chile trench induced by plate flexure. Geochem. J. 47, 249–257.

Hirano, N., Takahashi, E., Yamamoto, J., Machida, S., Abe, N., Ingle, S., Kaneoka, I., Hirata, T., Kimura, J., Ishii, T., Ogawa, Y., 2006. Volcanism in response to plate flexure. Science 313, 1426–1428.

Hirschmann, M. M., 2010. Partial melt in the oceanic low velocity zone. Phys. Earth Planet. Inter. 179, 60–71.

Hirschmann, M. M., Stolper, E. M., 1996. A possible role for garnet pyroxenite in the origin of the ”garnet signature” in MORB. Contrib. Mineral. Petrol. 124, 185–208.

Hirth, G., Kohlstedt, D., 2003. Rheology of the upper mantle and the mantle wedge: A view from the experimentalists. In: Eiler, J. (Ed.), Inside the Subduction Factory. American Geophysical Union, Washington, DC, pp. 83–105.

Hirth, G., Kohlstedt, D. L., 1995. Experimental constraints on the dynamics of the partially molten upper mantle: Deformation in the diffusion creep regime. J. Geophys. Res. 100, 1981–2001.

Hirth, G., Kohlstedt, D. L., 1996. Water in the oceanic mantle: Implications for rheology, melt extraction, and the evolution of the lithosphere. Earth Planet. Sci. Lett. 144, 93–108.

Hofmann, A. W., 1988. Chemical differentiation of the Earth: the relationship between mantle, continental crust, and oceanic crust. Earth Planet. Sci. Lett. 90, 297–314.

Hofmann, A. W., 1997. Mantle geochemistry: The message from oceanic volcanism. Nature 385, 219–229.

Hoggard, M. J., Winterbourne, J., Czarnota, K., White, N., 2017. Oceanic residual depth measurements, the plate cooling model, and global dynamic topography. J. Geophys. Res. Solid Earth 122, 2328–2372, doi:10.1002/2016JB013457.

Holland, H. D., 2002. Volcanic gases, black smoker, and the great oxidation event. Geochim. Cosmochim. Acta 66, 3811–3826.

Huang, J., Zhong, S., 2005. Sublithospheric small-scale convection and its implications for residual topography at old ocean basins and the plate model. J. Geophys. Res. 110, B05404, 10.1029/2004JB003153.

Huang, J., Zhong, S., Hunen, J. v., 2003. Controls on sublithospheric small-scale convection. J. Geophys. Res. 108 (B8), 2405, doi:10.1029/2003JB002456.

Idrissi, H., Bollinger, C., Boioli, F., Schryvers, D., Cordier, P., 2016. Low-temperature plasticity of olivine revisited with in situ TEM nanomechanical testing. Sci. Adv. 2, e1501671.

Isacks, B., Oliver, J., Sykes, L. R., 1968. Seismology and the new global tectonics. J. Geophys. Res. 73, 5855–5899.

Isse, T., Kawakatsu, H., Yoshizawa, K., Takeo, A., Shiobara, H., Sugioka, H., Ito, A., Suetsugu, D., Reymond, D., 2019. Surface wave tomography for the Pacific Ocean incorporating seafloor seismic observations and plate thermal evolution. Earth Planet. Sci. Lett. 510, 116–130.

Ito, E., Harris, D. M., Anderson, A. T., 1983. Alteration of oceanic crust and geologic cycling of chlorine and water. Geochim. Cosmochim. Acta 47, 1613–1624.

Ito, G., Mahoney, J. J., 2005a. Flow and melting of a heterogeneous mantle: 1. method and importance to the geochemistry of ocean island and mid-ocean ridge basalts. Earth Planet. Sci. Lett. 230, 29–46.

Ito, G., Mahoney, J. J., 2005b. Flow and melting of a heterogeneous mantle: 2. implications for a chemically nonlayered mantle. Earth Planet. Sci. Lett. 230, 47–63.

Ivandic, M., Grevemeyer, I., Berhort, A., Flueh, E. R., McIntosh, K., 2008. Impact of bending related faulting on the seismic properties of the incoming oceanic plate offshore of Nicaragua. J. Geophys. Res. 113, B05410, doi:10.1029/2007JB005291.

Jacobsen, S. B., 1988. Isotopic constraints on crustal growth and recyling. Earth Planet. Sci. Lett. 90, 315–329.

Jaeger, J. C., Cook, N. G. W., 1976. Fundamentals of Rock Mechanics. Chapman & Hall, London.

Jaffres, J. B. D., Shields, G. A., Wallmann, K., 2007. The oxygen isotope evolution of seawater: A critical review of a long-standing controversy and an improved geological water cycle for the past 3.4 billion years. Earth Sci. Rev. 83, 83–122.

Jain, C., Korenaga, J., Karato, S., 2017. On the yield strength of oceanic lithosphere. Geophys. Res. Lett. 44, 9716–9722, https://doi.org/10.1002/2017GL075043.

Jain, C., Korenaga, J., Karato, S., 2018. On the grain-size sensitivity of olivine rheology. J. Geophys. Res. Solid Earth 123, 674–688, https://doi.org/10.1002/2017JB014847.

Jain, C., Korenaga, J., Karato, S., 2019. Global analysis of experimental data on the rheology of olivine aggregates. J. Geophys. Res. Solid Earth 124, 310–334, https://doi.org/10.1029/2018JB016558.

Jarrard, R. D., 2003. Subduction fluxes of water, carbon dioxide, chlorine, and potassium. Geochem. Geophys. Geosys. 4, 8905, doi:10.1029/2002GC000392.

Jaupart, C., Mareschal, J.-C., 2015. Heat flow and thermal structure of the lithosphere. In: Treatise on Geophysics, 2nd ed. Vol. 6. Elsevier, pp. 217–253.

Johnson, B. W., Wing, B. A., 2020. Limited Archean continental emergencec reflected in an early Archean ^{18}O-enriched ocean. Nature Geosci. 13, 243–248.

Jung, H., Katayama, I., Jiang, Z., Hiraga, T., Karato, S., 2006. Effect of water and stress on the lattice-preferred orientation of olivine. Tectonophysics 421, 1–22.

Kameyama, M., Yuen, D., Fujimoto, H., 1997. The interaction of viscous heating with grain-size dependent rheology in the formation of localized slip zones. Geophys. Res. Lett. 24, 2523–2526.

Kaneshima, S., Helffrich, G., 1998. Detection of lower mantle scatterers northeast of the Mariana subduction zone using short-period array data. J. Geophys. Res. 103, 4825–4838.

Karato, S., 1986. Does partial melting reduce the creep strength of the upper mantle? Nature 319, 309–310.

Karato, S., 2008. Deformation of Earth Materials: Introduction to the Rheology of the Solid Earth. Cambridge, New York.

Karato, S., 2010. Rheology of the Earth's mantle: A historical review. Gondwana Res. 18, 17–45.

Karato, S., 2012. On the origin of the athenosphere. Earth Planet. Sci. Lett. 321-322, 95–103.

Karato, S., Barbot, S., 2018. Dynamcs of fault motion and the origin of contrasting tectonic style between Earth and Venus. Sci. Rep. 8, 11884, doi:10.1038/s41598–018–30174–6.

Karato, S., Olugboji, T., Park, J., 2015. Mechanisms and geologic significance of the mid-lithosphere discontinuity in the continents. Nature Geosci. 8, 509–514.

Karato, S., Paterson, M. S., FitzGerald, J. D., 1986. Rheology of synthetic olivine aggregates: Influence of grain size and water. J. Geophys. Res. 91, 8151–8176.

Karato, S., Wu, P., 1993. Rheology of the upper mantle: A synthesis. Science 260, 771–778.

Karato, S.-I., 1998. Micro-physics of post glacial rebound. GeoResearch Forum 3-4, 351–364.

Kasting, J. F., 2013. What caused the rise of atmospheric O_2? Chem. Geol. 362, 13–25.

Kasting, J. F., Catling, D., 2003. Evolution of a habitable planet. Annu. Rev. Astron. Astrophys. 41, 429–463.

Katayama, I., Karato, S., 2008. Low-temperature, high-stress deformation of olivine under water-saturated conditions. Phys. Earth Planet. Inter. 168, 125–133.

Katzman, R., Zhao, L., Jordan, T. H., 1998. High-resolution, two-dimensional vertical tomography of the central Pacific mantle using ScS reverberations and frequency-dependent travel times. J. Geophys. Res. 103, 17933–17971.

Kaufmann, G., Lambeck, K., 2000. Mantle dynamics, postglacial rebound and radial viscosity profile. Phys. Earth Planet. Inter. 121, 301–324.

Kawakatsu, H., Kumar, P., Takei, Y., Shinohara, M., Kanazawa, T., Araki, E., Suyehiro, K., 2009. Seismic evidence for sharp lithosphere-asthenosphere boundaries of oceanic plates. Science 324, 499–502.

Kawakatsu, H., Utada, H., 2017. Seismic and electrical signatures of the lithosphere-asthenosphere system of the normal oceanic mantle. Annu. Rev. Earth Planet. Sci. 45, 139–167.

Kawazoe, T., Karato, S., Otsuka, K., Jing, Z., Mookherjee, M., 2009. Shear deformation of dry polycrystalline olivine under deep upper mantle conditions using a rotational Drickamer apparatus (RDA). Phys. Earth Planet. Inter. 174, 128–137.

Kelemen, P. B., Hart, S. R., Bernstein, S., 1998. Silica enrichment in the continental upper mantle via melt/rock reaction. Earth Planet. Sci. Lett. 164, 387–406.

Kennett, B. L. N., Furumura, T., Zhao, Y., 2014. High-frequency Po/So guided waves in the oceanic lithosphere: II — heterogeneity and attenuation. Geophys. J. Int. 199, 614–630.

King, S. D., 1995. Models of mantle viscosity. In: Global Earth Physics: A Handbook of Physical Constants. American Geophysical Union, pp. 227–236.

King, S. D., Adam, C., 2014. Hotspot swells revisited. Phys. Earth Planet. Inter. 235, 66–83.

Kirby, S. H., 1985. Rock mechanics observations pertinent to the rheology of the continental lithosphere and the localization of strain along shear zones. Tectonophysics 119, 1–27.

Kita, S., Okada, T., Hasegawa, A., Nakajima, J., Matsuzawa, T., 2010. Existence of interplane earthquakes and neutral stress boundary between the upper and lower planes of the double seismic zone beneath Tohoku and Hokkaido, northeastern Japan. Tectonophysics 496, 68–82.

Klein, E. M., Langmuir, C. H., 1987. Global correlations of ocean ridge basalt chemistry with axial depth and crustal thickness. J. Geophys. Res. 92, 8089–8115.

Kneller, E. A., van Keken, P. E., Karato, S., Park, J., 2005. B-type olivine fabric in the mantle wedge: Insights from high-resolution non-Newtonian subduction zone models. Earth Planet. Sci. Lett. 237, 781–797.

Kohlstedt, D. L., Evans, B., Mackwell, S. J., 1995. Strength of the lithosphere: Constraints imposed by laboratory experiments. J. Geophys. Res. 100, 17658–17602.

Kohlstedt, D. L., Mackwell, S. J., 2009. Strength and deformation of planetary lithospheres. In: Watters, T. R., Schultz, R. A. (Eds.), Planetary Tectonics. Cambridge Univ. Press, pp. 397–456.

Korenaga, J., 2005a. Firm mantle plumes and the nature of the core-mantle boundary region. Earth Planet. Sci. Lett. 232, 29–37.

Korenaga, J., 2005b. Why did not the Ontong Java Plateau form subaerially? Earth Planet. Sci. Lett. 234, 385–399.

Korenaga, J., 2006. Archean geodynamics and the thermal evolution of Earth. In: Benn, K., Mareschal, J.-C., Condie, K. (Eds.), Archean Geodynamics and Environments. American Geophysical Union, Washington, D.C., pp. 7–32.

Korenaga, J., 2007a. Effective thermal expansivity of Maxwellian oceanic lithosphere. Earth Planet. Sci. Lett. 257, 343–349.

Korenaga, J., 2007b. Thermal cracking and the deep hydration of oceanic lithosphere: A key to the generation of plate tectonics? J. Geophys. Res. 112, B05408, doi:10.1029/2006JB004502.

Korenaga, J., 2009. How does small-scale convection manifest in surface heat flux? Earth Planet. Sci. Lett. 287, 329–322.

Korenaga, J., 2010. Scaling of plate-tectonic convection with pseudoplastic rheology. J. Geophys. Res. 115, B11405, doi:10.1029/2010JB007670.

Korenaga, J., 2011a. Thermal evolution with a hydrating mantle and the initiation of plate tectonics in the early Earth. J. Geophys. Res. 116, B12403, doi:10.1029/2011JB008410.

Korenaga, J., 2011b. Velocity-depth ambiguity and the seismic structure of large igneous provinces: A case study from the Ontong Java Plateau. Geophys. J. Int. 185, 1022–1036.

Korenaga, J., 2013. Initiation and evolution of plate tectonics on Earth: Theories and observations. Annu. Rev. Earth Planet. Sci. 41, 117–151.

Korenaga, J., 2015a. Constraining the geometries of small-scale heterogeneities: A case study from the Mariana region. J. Geophys. Res. 120, 7830–7851, doi:10.1002/2015JB012432.

Korenaga, J., 2015b. Seafloor topography and the thermal budget of Earth. In: Foulger, G. R., Lustrino, M., King, S. D. (Eds.), The Interdisciplinary Earth: A Volume in Honor of Don L. Anderson. GSA Special Paper 514 and AGU Special Publication 71. Geological Society of America, pp. 167–185.

Korenaga, J., 2017a. On the extent of mantle hydration by plate bending. Earth Planet. Sci. Lett. 457, 1–9.

Korenaga, J., 2017b. Pitfalls in modeling mantle convection with internal heating. J. Geophys. Res. Solid Earth 122, 4064–4085, doi:10.1002/2016JB013850.

Korenaga, J., 2018. Crustal evolution and mantle dynamics through Earth history. Phil. Trans. R. Soc. A 376, 20170408, http://dx.doi.org/10.1098/rsta.2017.0408.

Korenaga, J., Jordan, T. H., 2002a. On 'steady-state' heat flow and the rheology of oceanic mantle. Geophys. Res. Lett. 29 (22), 2056, doi:10.1029/2002GL016085.

Korenaga, J., Jordan, T. H., 2002b. Onset of convection with temperature- and depth-dependent viscosity. Geophys. Res. Lett. 29 (19), 1923, doi:10.1029/2002GL015672.

Korenaga, J., Jordan, T. H., 2003. Physics of multiscale convection in Earth's mantle: Onset of sublithospheric convection. J. Geophys. Res. 108 (B7), 2333, doi:10.1029/2002JB001760.

Korenaga, J., Jordan, T. H., 2004. Physics of multiscale convection in Earth's mantle: Evolution of sublithospheric convection. J. Geophys. Res. 109, B01405, doi:10.1029/2003JB002464.

Korenaga, J., Karato, S., 2008. A new analysis of experimental data on olivine rheology. J. Geophys. Res. 113, B02403, doi:10.1029/2007JB005100.

Korenaga, J., Kelemen, P. B., 2000. Major element heterogeneity of the mantle source in the North Atlantic igneous province. Earth Planet. Sci. Lett. 184, 251–268.

Korenaga, J., Kelemen, P. B., Holbrook, W. S., 2002. Methods for resolving the origin of large igneous provinces from crustal seismology. J. Geophys. Res. 107 (B9), 2178, doi:10.1029/2001JB001030.

Korenaga, J., Planavsky, N. J., Evans, D. A. D., 2017. Global water cycle and the coevolution of Earth's interior and surface environment. Phil. Trans. R. Soc. A 375, 20150393, doi:10.1098/rsta.2015.0393.

Korenaga, J., Sager, W. W., 2012. Seismic tomography of Shatsky Rise by adaptive importance sampling. J. Geophys. Res. 117, B08102, doi:10.1029/2012JB009248.

Korenaga, T., Korenaga, J., 2008. Subsidence of normal oceanic lithosphere, apparent thermal expansivity, and seafloor flattening. Earth Planet. Sci. Lett. 268, 41–51.

Korenaga, T., Korenaga, J., 2016. Evolution of young oceanic lithosphere and the meaning of seafloor subsidence rate. J. Geophys. Res. Solid Earth 121, 6315–6332, doi:10.1002/2016JB013395.

Kranz, R. L., 1983. Microcrakcs in rocks: A review. Tectonophysics 100, 449–480.

Kreemer, C., Gordon, R. G., 2014. Pacific plate deformation from horizontal thermal contraction. Geology 42, 847–850.

Kumamoto, K. M., Thom, C. A., Wallis, D., Hansen, L. N., Armstrong, D. E., Warren, J. M., Goldsby, D. L., Wilkinson, A. J., 2017. Size effects resolve discrepancies in 40 years of work on low-temperature plasticitiy in olivine. Sci. Adv. 3, e1701338.

Labrosse, S., 2002. Hotspots, mantle plumes and core heat loss. Earth Planet. Sci. Lett. 199, 147–156.

Lachenbruch, A. H., 1961. Depth and spacing of tension cracks. J. Geophys. Res. 66, 4273–4292.

Landuyt, W., Bercovici, D., 2009. Variations in planetary convection via the effect of climate on damage. Earth Planet. Sci. Lett. 277, 29–37.

Landuyt, W., Bercovici, D., Ricard, Y., 2008. Plate generation and two-phase damage theory in a model of mantle convection. Geophys. J. Int. 174, 1065–1080.

Langmuir, C. H., Klein, E. M., Plank, T., 1992. Petrological systematics of mid-ocean ridge basalts: Constraints on melt generation beneath ocean ridges. In: Phipps Morgan, J., Blackman, D. K., Sinton, J. M. (Eds.), Mantle Flow and Melt Generation at Mid-Ocean Ridges. Vol. 71 of Geophys. Monogr. Ser. AGU, Washington, D. C., pp. 183–280.

Langseth, M. G., Le Pichon, X., Ewing, M., 1966. Crustal structure of the mid-ocean ridges, 5, heat flow through the Atlantic ocean floor and convection currents. J. Geophys. Res. 71, 5321–5355.

Lay, T., Hernlund, J., Buffett, B. A., 2008. Core-mantle boundary heat flow. Nature Geosci. 1, 25–32.

Lenardic, A., Jellinek, A. M., Moresi, L.-N., 2008. A climate induced transition in the tectonic style of a terrestrial planet. Earth Planet. Sci. Lett. 271, 34–42.

Lin, P.-Y. P., Gaherty, J. B., Jin, G., Collins, J. A., Lizarralde, D., Evans, R. L., Hirth, G., 2016. High-resolution seismic constraints on flow dynamics in the oceanic asthenosphere. Nature 535, 538–541.

Linckens, J., Bruijn, R. H. C., Skemer, P., 2014. Dynamic recrystallization and phase mixing in experimentaly deformed peridotite. Earth Planet. Sci. Lett. 388, 134–142.

Lister, C. R. B., 1974. On the penetration of water into hot rock. Geophys. J. R. Astron. Soc. 39, 465–509.

Lizarralde, D., Gaherty, J. B., Collins, J. A., Hirth, G., Kim, S. D., 2004. Spreading-rate dependence of melt extraction at mid-ocean ridges from mantle seismic refraction data. Nature 432, 744–747.

Long, H., Weidner, D. J., Li, L., Chen, J., Wang, L., 2011. Deformation of olivine at subduction zone conditions determined from *in situ* measurements with synchrotron radiation. Phys. Earth Planet. Inter. 186, 23–35.

Maggi, A., Debayle, E., Priestley, K., Barruol, G., 2006. Multimode surface waveform tomography of the Pacific Ocean: a closer look at the lithospheric cooling signature. Geophys. J. Int. 166, 1384–1397.

Magni, V., Bouihol, P., van Hunen, J., 2014. Deep water recycling through time. Geochem. Geophys. Geosys. 15, 4203–4216, doi:10.1002/2014GC005525.

Mahoney, J., Fitton, J., Wallace, P., the Shipboard Scientific Party, 2001. Proceedings of the Ocean Drilling Program Initial Report vol. 192. Ocean Drilling Program, College Station, TX.

Manga, M., 1996. Mixing of heterogeneities in the mantle: Effect of viscosity differences. Geophys. Res. Lett. 23, 403–406.

Margerin, L., Nolet, G., 2003. Multiple scattering of high-frequency seismic waves in the deep Earth: *PKP* precursor analysis and inversion for mantle granularity. J. Geophys. Res. 108, 2514, doi:10.1029/2003JB002455.

Masuti, S., Barbot, S., Karato, S., Feng, L., Banerjee, P., 2016. Upper-mantle water stratification inferred from observations of the 2012 Indian Ocean earthquake. Nature 538, 373–377.

McCarthy, C., Takei, Y., Hiraga, T., 2011. Experimental study of attenuation and dispersion over a broad frequency range, 2, the universal scaling of polycrystalline materials. J. Geophys. Res. 116, B09207, doi:10.1029/2011JB008384.

McKenzie, D., Bickle, M. J., 1988. The volume and composition of melt generated by extension of the lithosphere. J. Petrol. 29, 625–679.

McKenzie, D., Jackson, J., Priestley, K., 2005. Thermal structure of oceanic and continental lithosphere. Earth Planet. Sci. Lett. 233, 337–349.

McKenzie, D. P., 1967. Some remarks on heat flow and gravity anomalies. J. Geophys. Res. 72, 6261–6273.

Mei, S., Kohlstedt, D. L., 2000a. Influence of water on plastic deformation of olivine aggregates, 1, diffusion creep regime. J. Geophys. Res. 105, 21457–21469.

Mei, S., Kohlstedt, D. L., 2000b. Influence of water on plastic deformation of olivine aggregates, 2, dislocation creep regime. J. Geophys. Res. 105, 21471–21481.

Mei, S., Suzuki, A. M., Kohlstedt, D. L., Dixon, N. A., Durham, W. B., 2010. Experimental constraints on the strength of the lithospheric mantle. J. Geophys. Res. 115, B08204, doi:10.1029/2009JB006873.

Michael, P. J., 1999. Implications for magmatic processes at Ontong Java Plateau from volatile and major element contents of Cretaceous basalt glasses. Geochem. Geophys. Geosys. 1, 1999GC000025.

Mitrovica, J. X., Forte, A. M., 2004. A new inference of mantle viscosity based upon joint inversion of convection and glacial isostatic adjustment data. Earth Planet. Sci. Lett. 225, 177–189.

Miura, S., Suyehiro, K., Shinohara, M., Takahashi, N., Araki, E., Taira, A., 2004. Seismological structure and implications of collision between the Ontong Java Plateau and Solomon Island Arc from ocean bottom seismometer-airgun data. Tectonophysics 389, 191–220.

Miyashiro, A., 1973. The Troodos ophiolite complex was probably formed in an island arc. Earth Planet. Sci. Lett. 19, 218–224.

Moresi, L., Solomatov, V., 1998. Mantle convection with a brittle lithosphere: thoughts on the global tectonic styles of the Earth and Venus. Geophys. J. Int. 133, 669–682.

Morgan, W. J., 1971. Convection plumes in the lower mantle. Nature 230, 42–43.

Muki, R., Sternberg, E., 1961. On transient thermal stresses in viscoelastic materials with temperature-dependent properties. Journal of Applied Mechanics 28, 193–207.

Mullet, B. G., Korenaga, J., Karato, S.-I., 2015. Markov chain Monte Carlo inversion for the rheology of olivine single crystals. J. Geophys. Res. Solid Earth 120, 3142–3172, doi:10.1002/2014JB011845.

Mulyukova, E., Bercovici, D., 2018. Collapse of passive margins by lithospheric damage and plunging grain size. Earth Planet. Sci. Lett. 484, 341–352.

Naif, S., Key, K., Constable, S., Evans, R. L., 2015. Water-rich bending faults at the Middle America Trench. Geochem. Geophys. Geosys. 16, doi:10.1002/2015GC005927.

Nakagawa, T., Tackley, P. J., 2005. Deep mantle heat flow and thermal evolution of the Earth's core in thermochemical multiphase models of mantle convection. Geochem. Geophys. Geosys. 6, Q08003, doi:10.1029/2005GC000967.

Nakagawa, T., Tackley, P. J., 2012. Influence of magmatism on mantle cooling, surfae heat flow and Urey ratio. Earth Planet. Sci. Lett. 329-330, 1–10.

Ohuchi, T., Kawazoe, T., Higo, Y., Funakoshi, H., Suzuki, A., Kikegawa, T., Irifune, T., 2015. Dislocation-accomodated grain boundary sliding as the major deformation mechanism of olivine in the Earth's upper mantle. Sci. Adv. 1, e1500360.

Olive, J.-A., Behn, M. D., Tucholke, B. E., 2010. The structure of oceanic core complexes controlled by the depth distribution of magma emplacement. Nature Geosci. 3, 491–495.

Olson, P., Yuen, D. A., Balsigar, D., 1984. Convective mixing and the fine structure of mantle heterogeneity. Earth Planet. Sci. Lett. 36, 291–304, very good paper!

O'Neill, C., Lenardic, A., Moresi, L., Torsvik, T. H., Lee, C.-T., 2007. Episodic Precambrian subduction. Earth Planet. Sci. Lett. 262, 552–562.

O'Neill, C., Lenardic, A., Weller, M., Moresi, L., Quenette, S., Zhang, S., 2016. A window for plate tectonics in terrestrial planet evolution? Phys. Earth Planet. Inter. 255, 80–92.

O'Neill, C., Marchi, S., Zhang, S., Bottke, W., 2017. Impact-driven subduction on the Hadean Earth. Nature Geosci. 10, 793–797.

O'Rourke, J. G., Korenaga, J., Stevenson, D. J., 2017. Thermal evolution of Earth with magnesium precipitation in the core. Earth Planet. Sci. Lett. 458, 263–272.

Panet, I., Pollitz, F., Mikhailov, V., Diament, M., Banerjee, P., Grijalva, K., 2010. Upper mantle rheology from GRACE and GPS postseismic deformation after the 2004 Sumatra-Andeman earthquake. Geochem. Geophys. Geosys. 11, Q06008, doi:10.1029/2009GC002905.

Parai, R., Mukhopadhyay, S., 2012. How large is the subducted water flux? new constraints on mantle regassing rates. Earth Planet. Sci. Lett. 317-318, 396–406.

Parsons, B., McKenzie, D., 1978. Mantle convection and the thermal structure of the plates. J. Geophys. Res. 83, 4485–4496.

Parsons, B., Sclater, J. G., 1977. An analysis of the variation of ocean floor bathymetry and heat flow with age. J. Geophys. Res. 82 (5), 803–827.

Paterson, M. S., Wong, T.-F., 2005. Experimental Rock Deformation — The Brittle Field. Springer.

Phipps Morgan, J., Morgan, W. J., Price, E., 1995. Hotspot melting generates both hotspot volcanism and a hotspot swell? J. Geophys. Res. 100, 8045–8062.

Pollack, H. N., Hurter, S. J., Johnson, J. R., 1993. Heat flow from the Earth's interior: Analysis of the global data set. Rev. Geophys. 31, 267–280.

Pollitz, F. F., 2003. Transient rheology of the uppermost mantle beneath the Mojave Desert, California. Earth Planet. Sci. Lett. 215, 89–104.

Priestley, K., McKenzie, D., 2013. The relationship between shear wave velocity, temperature, attenuation and viscosity in the shallow part of the mantle. Earth Planet. Sci. Lett. 381, 78–91.

Proietti, A., Bystricky, M., Guignard, J., Béjina, F., Crichton, W., 2016. Effect of pressure on the strength of olivine at room temperature. Phys. Earth Planet. Inter. 259, 34–44.

Raddick, M. J., Parmentier, E. M., Scheirer, D. S., 2002. Buoyant decompression melting: A possible mechanism for intraplate volcanism. J. Geophys. Res. 107, 2228, doi:.10.1029/2001JB000617.

Rampino, M. R., Caldeira, K., 1994. The Goldilocks problem: Climatic evolution and long-term habitability of terrestrial planets. Annu. Rev. Astron. Astrophys. 32, 83–114.

Ranero, C. R., Morgan, J. P., McIntosh, K., Reichert, C., 2003. Bending-related faulting and mantle serpentinization at the Middle America trench. Nature 425, 367–373.

Rempel, A. W., Rice, J. R., 2006. Thermal pressurization and onset of melting in fault zones. J. Geophys. Res. 111, B09314, doi:10.1029/2006JB004314.

Rey, P. F., Coltice, N., Flament, N., 2014. Spreading continents kick-started plate tectonics. Nature 513, 405–408.

Ribe, N. M., Christensen, U. R., 1994. Three-dimensional modeling of plume-lithosphere interaction. J. Geophys. Res. 99, 669–682.

Ribe, N. M., Christensen, U. R., 1999. The dynamical origin of Hawaiian volcanism. Earth Planet. Sci. Lett. 171, 517–531.

Rice, J. R., 2006. Heating and weakening of faults during earthquake slip. J. Geophys. Res. 111, B05311, doi:10.1029/2005JB004006.

Richards, F. D., Hoggard, M. J., Cowton, L. R., White, N. J., 2018. Reassessing the thermal structure of oceanic lithosphere with revised global inventories of basement depths and heat flow measurements. J. Geophys. Res. Solid Earth 123, 9136–9161, https://doi.org/10.1029/2018JB015998.

Richards, M., Contreras-Reyes, E., Lithgow-Bertelloni, C., Ghiorso, M., 2013. Petrological interpretation of deep crustal intrusive bodies beneath oceanic hotspot provinces. Geochem. Geophys. Geosys. 14, 604–619, doi:10.1029/2012GC004448.

Richards, M. A., Duncan, R. A., Courtillot, V. E., 1989. Flood basalts and hot-spot tracks: Plume heads and tails. Science 246, 103–107.

Richards, M. A., Yang, W.-S., Baumgardner, J. R., Bunge, H.-P., 2001. Role of a low-viscosity zone in stabilizing plate tectonics: Implications for comparative terrestrial planetology. Geochem. Geophys. Geosys. 2, 2000GC000115.

Richardson, W. P., Stein, S., Stein, C. A., Zuber, M. T., 1995. Geoid data and thermal structure of the oceanic lithosphere. Geophys. Res. Lett. 22, 1913–1916.

Ringwood, A. E., 1975. Compositions and petrology of the Earth's mantle. McGraw-Hill, New York.

Ritzwoller, M. H., Shapiro, N. M., Zhong, S., 2004. Cooling history of the Pacific lithosphere. Earth Planet. Sci. Lett. 226, 69–84.

Roberge, J., Wallace, P. J., White, R. V., Coffin, M. F., 2005. Anomalous uplift and subsidence of the Ontong Java Plateau inferred from CO_2 contents of submarine basaltic glasses. Geology 33, 501–504.

Rosas, J. C., Korenaga, J., 2018. Rapid crustal growth and efficient crustal recycling in the early Earth: Implications for Hadean and Archean geodynamics. Earth Planet. Sci. Lett. 494, 42–49.

Rudolph, M. L., Lekic, V., Lithgow-Bertelloni, C., 2015. Viscosity jump in Earth's mid-mantle. Science 350, 1349–1352.

Rüpke, L. H., Phipps Morgan, J., Hort, M., Connolly, J. A. D., 2004. Serpentine and the subduction zone water cycle. Earth Planet. Sci. Lett. 223, 17–34.

Rychert, C. A., Shearer, P. M., 2011. Imaging the lithosphere-asthenosphere boundary beneath the Pacific using *SS* waveform modeling. J. Geophys. Res. 116, B07307, doi:10.1029/2010JB008070.

Sallares, V., Charvis, P., Flueh, E. R., Bialas, J., Party, T. S. S., 2005. Seismic structure of the Carnegie ridge and the nature of the Galapagos hotspot. Geophys. J. Int. 161, 763–788.

Sandwell, D., Fialko, Y., 2004. Warping and cracking of the Pacific plate by thermal contraction. J. Geophys. Res. 109, B10411, doi:10.1029/2004JB003091.

Sarafian, E., Evans, R. L., Collins, J. A., Elsenbeck, J., Gaetani, G. A., Gaherty, J. B., Hirth, G., Lizarralde, D., 2015. The electrical structure of the central Pacific upper mantle constrained by the NoMelt experiment. Geochem. Geophys. Geosys. 16, 1115–1132, doi:10.1002/2014GC005709.

Schmerr, N., 2012. The Gutenberg discontinuity: Melt at the lithosphere-asthenosphere boundary. Science 335, 1480–1483.

Scholz, C. H., 2002. The Mechanics of Earthquakes and Faulting, 2nd ed. Cambridge Univ. Press.

Schroeder, W., 1984. The empirical age-depth relation and depth anomalies in the Pacific ocean basin. J. Geophys. Res. 89, 9873–9883.

Schubert, G., Turcotte, D. L., Olson, P., 2001. Mantle Convection in the Earth and Planets. Cambridge, New York.

Searle, M., Cox, J., 1999. Tectonic setting, origin, and obduction of the Oman ophiolite. GSA Bulletin 111, 104–122.

Servali, A., Korenaga, J., 2018. Oceanic origin of continental mantle lithosphere. Geology 46, 1047–1059.

Shito, A., Suetsugu, D., Furumura, T., 2015. Evolution of the oceanic lithosphere inferred from Po/So waves travelling in the Philippine Sea Plate. J. Geophys. Res. Solid Earth 120, 5238–5248, doi:.10.1002/2014JB011814.

Shito, A., Suetsugu, D., Furumura, T., Sugioka, H., Ito, A., 2013. Small-scale heterogeneities in the oceanic litho- sphere inferred from guided waves. Geophys. Res. Lett. 40, 1708–1712.

Shizgal, B. D., Arkos, G. G., 1996. Nonthermal escape of the atmospheres of Venus, Earth, and Mars. Rev. Geophys. 34, 483–505.

Sifre, D., Gardes, E., Massuyeau, M., Hashim, L., Hier-Majumder, S., Gaillard, F., 2014. Electrial conductivity during incipient melting in the oceanic low-velocity zone. Nature 509, 81–85.

Simmons, G., Richter, D., 1976. Microcracks in rock. In: Strens, R. G. J. (Ed.), The Physics and Chemistry of Minerals and Rocks. Wiley, pp. 105–137.

Sizova, E., Gerya, T., Brown, M., Perchuk, L. L., 2010. Subduction styles in the Precambrian: Insight from numerical experiments. Lithos 116, 209–229.

Sleep, N. H., 1987. Lithospheric heating by mantle plumes. Geophys. J. R. Astron. Soc. 91, 1–12.

Sleep, N. H., 1990. Hotspots and mantle plumes: some phenomenology. J. Geophys. Res. 95, 6715–6736.

Sleep, N. H., 2005. Dioxygen over geologic time. Metal Ions in Biological Systems 43, 49–73.

Smith, W. H. F., Sandwell, D. T., 1997. Global sea floor topography from satellite altimetry and ship depth soundings. Science 277, 1956–1962.

Sobolev, A. V., Hofmann, A. W., Kuzmin, D. V., Yaxley, G. M., Arndt, N. T., Chung, S.-L., Danyushevsky, L. V., Elliott, T., Frey, F. A., Garcia, M. O., Gurenko, A. A., Kamenetsky, V. S., Kerr, A. C., Krivolutskaya, N. A., Matvienkov, V. V., Nikogosian, I. K., Rocholl, A., Sigurdsson, I. A., Sushchevskaya, N. M., Teklay, M., 2007. The amount of recycled crust in sources of mantle-derived melts. Science 316, 412–417.

Solomatov, V. S., 1995. Scaling of temperature- and stress-dependent viscosity convection. Phys. Fluids 7, 266–274.

Solomatov, V. S., 1996. Can hotter mantle have a larger viscosity? Geophys. Res. Lett. 23, 937–940.

Solomatov, V. S., 2004. Initiation of subduction by small-scale convection. J. Geophys. Res. 109, B01412, doi:10.1029/2003JB002628.

Solomatov, V. S., Moresi, L.-N., 2000. Scaling of time-dependent stagnant lid convection: Application to small-scale convection on earth and other terrestrial planets. J. Geophys. Res. 105, 21795–21817.

Stadler, G., Gurnis, M., Burstedde, C., Wilcox, L. C., Alisic, L., Ghattas, O., 2010. The dynamics of plate tectonics and mantle flow: From local to global scales. Science 329, 1033–1038.

Stakes, D. S., Taylor, H. P., 1992. The northern Samail ophiolite: An oxygen isotope, microprobe, and field study. J. Geophys. Res. 97, 7043–7080.

Stein, C., Schmalzl, J., Hansen, U., 2004. The effect of rheological parameters on plate behavior in a self-consistent model of mantle convection. Phys. Earth Planet. Inter. 142, 225–255.

Stein, C. A., Stein, S., 1992. A model for the global variation in oceanic depth and heat flow with lithospheric age. Nature 359, 123–129.

Stein, C. A., Stein, S., 1994. Constraints on hydrothermal heat flux through the oceanic lithosphere from global heat flow. J. Geophys. Res. 99, 3081–3095.

Stern, T. A., Henrys, S. A., Okaya, D., Louie, J. N., Savag, M. K., Lamb, S., Sato, H., Sutherland, R., Iwasaki, T., 2015. A seismic reflection image for the base of a tectonic plate. Nature 518, 85–88.

Stevenson, D. J., Spohn, T., Schubert, G., 1983. Magnetism and thermal evolution of the terrestrial planets. Icarus 54, 466–489.

Stixrude, L., Lithgow-Bertelloni, C., 2005. Mineralogy and elasticity of the oceanic upper mantle: Origin of the low-velocity zone. J. Geophys. Res. 110, B03204, doi:10.1029/2004JB002965.

Tackley, P. J., Stevenson, D., 1993. A mechanism for spontaneous self-perpetuating volcanism on the terrestorial planets. In: Stone, D. B., Runcorn, S. K. (Eds.), Flow and Creep in the Solar System: Observations, Modeling and Theory. Kluwer Academic, pp. 307–321.

Takei, Y., 2017. Effects of partial melting on seismic velocity and attenuation: A new insight from experiments. Ann. Rev. Earth Planet. Sci. 45, 447–470, https://doi.org/10.1146/annurev–earth–063016–015820.

Takei, Y., Karasawa, F., Yamauchi, H., 2014. Temperature, grain size, and chemical controls on polycrystal anelasiticy over a broad frequency range extending into the seismic range. J. Geophys. Res. 119, 5414–5443, doi:10.1002/2014JB011146.

Takeo, A., Kawakatsu, H., Isse, T., Nishida, K., Shiobara, H., Sugioka, H., Ito, A., Utada, H., 2018. Is situ characterization of the lithosphere-asthenosphere system beneath NW Pacific Ocean broadband dispersion survey with two OBS arrays. Geochem. Geophys. Geosys. 19, https://doi.org/10.1029/2018GC007588.

Takeuchi, N., Kawakatsu, H., Shiobara, H., Isse, T., Sugioka, H., Ito, A., Utada, H., 2017. Determination of intrinsic attenuation in the oceanic lithosphere-asthenosphere system. Science 358 (1593-5196).

Trampert, J., Deschamps, F., Resovsky, J., Yuen, D., 2004. Probabilistic tomography maps chemical heterogeneities throughout the lower mantle. Science 306, 853–856.

Turcotte, D. L., 1974. Are transform faults thermal contraction cracks? J. Geophys. Res. 79, 2573–2577.

Turcotte, D. L., Oxburgh, E. R., 1967. Finite amplitude convective cells and continental drift. J. Fluid Mech. 28, 29–42.

Turcotte, D. L., Oxburgh, E. R., 1973. Mid-plate tectonics. Nature 244, 337–339.

Turcotte, D. L., Schubert, G., 1982. Geodynamics: Applications of Continuum Physics to Geological Problems, 2nd Edition. John Wiley, New York.

Wallmann, K., 2001. The geological water cycle and the evolution of marine δ^{18}O values. Geochim. Cosmochim. Acta 65, 2469–2485.

Watts, A. B., 2001. Isostasy and Flexure of the Lithosphere. Cambridge Univ. Press, New York.

Watts, A. B., ten Brink, U. S., Buhl, P., Brocher, T. M., 1985. A multichannel seismic study of lithospheric flexure across the Hawaiian-Emperor seamount chain. Nature 1985, 105–111.

Watts, A. B., Zhong, S., 2000. Observations of flexture and the rheology of oceanic lithosphere. Geophys. J. Int. 142, 855–875.

White, R. S., McKenzie, D., O'Nions, R. K., 1992. Oceanic crustal thickness from seismic measurements and rare earth element inversions. J. Geophys. Res. 97, 19683–19715.

Wilson, D. S., Teagle, D. A. H., Alt, J. C., Banerjee, N. R., Umino, S., Miyashita, S., Acton, G. D., Anma, R., Barr, S. R., Belghoul, A., Carlut, J., Christie, D. M., Coggon, R. M., Cooper, K. M., Cordier, C., Grispini, L., Durand, S. R., Einaudi, F., Galli, L., Gao, Y., Geldmacher, J., Gilbert, L. A., Hayman, N. W., Herrero-Bervera, E., Hirano, N., Holter, S., Ingle, S., Jiang, S., Kalberkamp, U., Kerneklian, M., Koepke, J., Laverne, C., Lledo Vasquez, H. L., Maclennan, J., Morgan, S., Neo, N., Nichols, H. J., Park, S., Reichow, M. K., Sakuyama, T., Sano, T., Sandwell, R., Scheibner, B., Smith-Duque, C. E., Swift, S. A., Tartarotti, P., Tikku, A. A., Tominaga, M., Veloso, E. A., Yamazaki, T., Yamazaki, S., Ziegler, C., 2006. Drilling to gabbro in intact ocean crust. Science 312, 1016–1020.

Winterbourne, J., White, N., Crosby, A., 2014. Accurate measurements of residual topography from the ocean realm. Tectonics 33, 982–1015, doi:10.1002:2013tC003372.

Yamamoto, J., Korenaga, J., Nirano, N., Kagi, H., 2014. Melt-rich lithosphere-asthenosphere boundary inferred from petit-spot volcanoes. Geology 42, 967–970.

Yamauchi, H., Takei, Y., 2016. Polycrystal anelasticity at nearsolidus temperatures. J. Geophys. Res. Solid Earth 121, 7790– 7820, https://doi.org/10.1002/2016JB013316.

Yasuda, A., Fujii, T., Kurita, K., 1994. Melting phase relations of an anhydrous mid-ocean ridge basalt from 3 to 20 GPa: Implications for the behavior of subducted oceanic crust in the mantle. J. Geophys. Res. 99, 9401–9414.

Zhong, S., 2006. Constraints on thermochemical convection of the mantle from plume heat flux, plume excess temperture, and upper mantle temperature. J. Geophys. Res. 111, B04409, doi:10.1029/2005JB003972.

Zhong, S., Watts, A. B., 2013. Lithospheric deformation induced by loading of the Hawaiian Islands and its implications for mantle rheology. J. Geophys. Res. 118, 6025–6048, doi:10.1002/2013JB010408.

Zindler, A., Hart, S., 1986. Chemical geodynamics. Annu. Rev. Earth Planet. Sci. 14, 493–571.

Table 1: Diffusion and dislocation creep parameters for olivine aggregates

Mechanism	Parameters[a]	Karato and Wu (1993)	Hirth and Kohlstedt (2003)	Jain et al. (2019)[b]
dry diffusion	A_3	$10^{9.38}$	$10^{9.18}$	$10^{7.86\pm0.15}$
	m_3	2.5	3	2.11 ± 0.15
	E_3	300	375 ± 50	370 ± 15
	V_3	6	2-10	–
wet diffusion	A_4	$10^{5.15}$	$10^{6.0}$	$10^{5.56\pm0.47}$
	m_4	2.5	3	1.74 ± 0.12
	r_4	-	1	0.84 ± 0.26
	E_4	240	335 ± 75	362 ± 60
	V_4	5	4	6.75 ± 13.23
dry dislocation	A_5	$10^{-1.22}$	$10^{5.04}$	$10^{2.10\pm0.20}$
	n_5	3.5	3.5 ± 0.3	3.64 ± 0.09
	E_5	540	530 ± 4	424 ± 23
	V_5	15-25	14-27	–
wet dislocation	A_6	$10^{1.0}$	$10^{1.95}$	$10^{-4.47\pm0.83}$
	n_6	3.0	3.5 ± 0.3	4.45 ± 0.32
	r_6	-	1.2	2.00 ± 0.02
	E_6	430	480 ± 40	425 ± 190
	V_6	10-20	11	27.96 ± 8.13

E_i are in kJ mol^{-1} and V_i are in cm^3 mol^{-1}.
[a]Parameter naming follows equations (3)-(10). The values of pre-exponential factors A_i assume that grain size is given in microns, stress in MPa, and water content in ppm H/Si.
[b]Listed are model OL-DB$_2$ for dry diffusion and dislocation creep and model OL-WB$_1$ for wet diffusion and dislocation creep (see Jain et al. (2019) for parameter covariance).

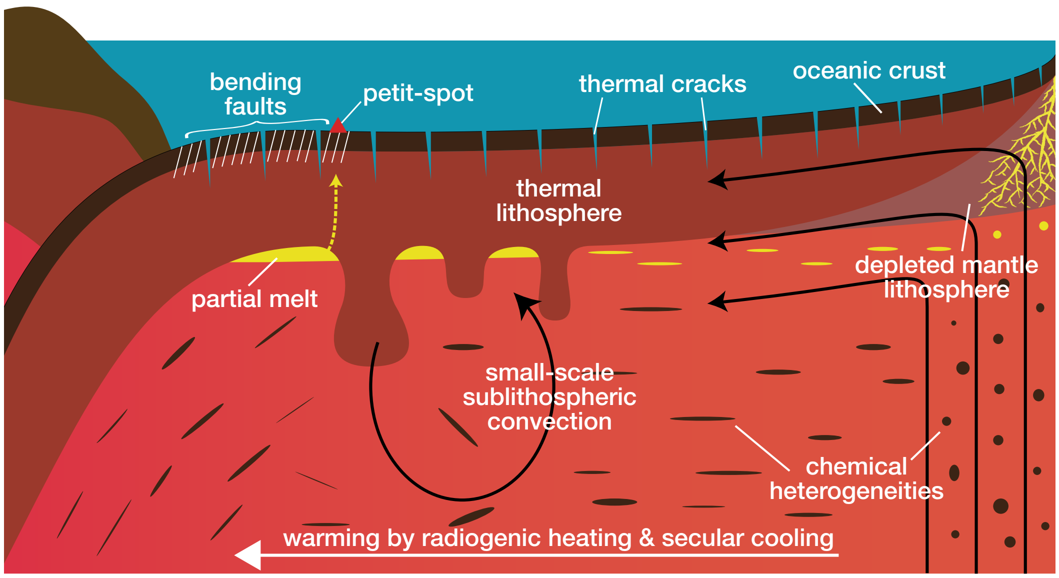

Figure 1: Schematic drawing for the evolution of 'normal' oceanic upper mantle (i.e., excluding the influence of perturbations from below such as mantle plumes). Partial melting associated with the upwelling beneath mid-ocean ridges creates oceanic crust as well as depleted mantle lithosphere. Thermal lithosphere grows by cooling from the above, and it eventually becomes convectively unstable, leading to the onset of small-scale sublithospheric convection. Preexisting chemical heterogeneities in the convecting mantle are stretched by corner flow, and some of them melt when brought to sufficiently shallow depths. Small-scale convection can further promote the partial melting of asthenospheric materials, and the ponding of partial melt beneath old lithosphere can result in the formation of petit-spot volcanos. The convecting mantle beneath older seafloor is slightly warmer owing to radiogenic heating and secular cooling. Thermal cracking gradually and pervasively hydrates oceanic lithosphere and also weakens it, with additional hydration brought by bending faults at subduction zones. All of these processes are discussed in this article. The illustration is not drawn to scale.

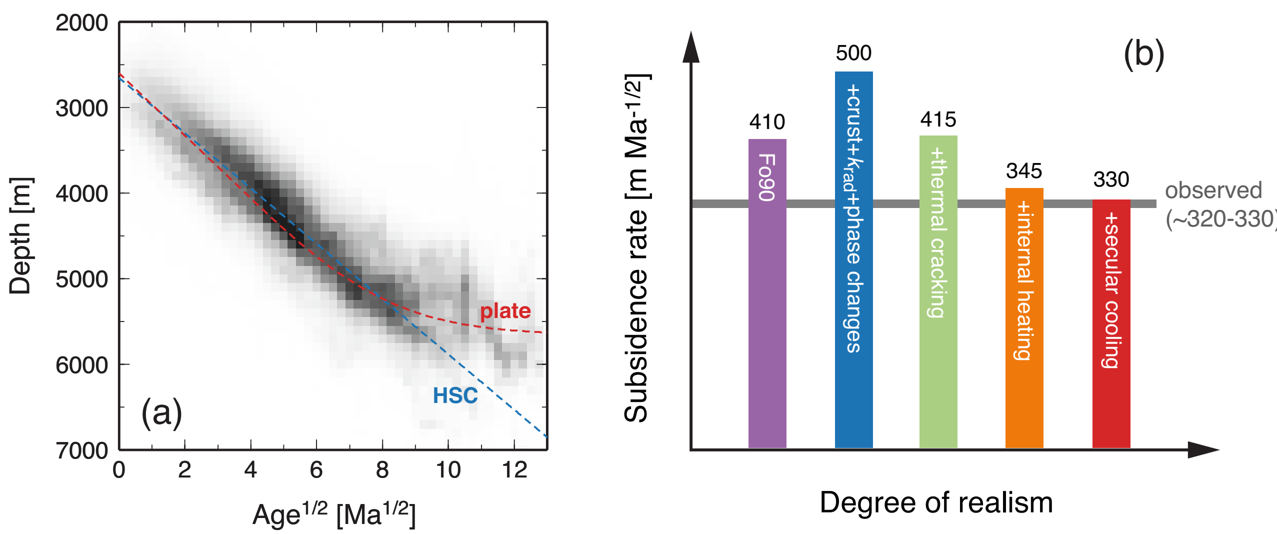

Figure 2: (a) Age-depth relation for the normal seafloor according to the correlation criterion of Korenaga and Korenaga (2008). Darker shading means larger area. Also shown are the predictions of the GDH1 plate model of Stein and Stein (1992) (red) and the best-fit half-space cooling trend, $2654 + 323\sqrt{t}$, where t is seafloor age in Ma, derived by Korenaga and Korenaga (2008) (blue). After Korenaga (2015b). (b) How predicted subsidence rate varies as more realistic complications are incorporated, based on the calculations ofKorenaga and Korenaga (2016) . "Fo90" (purple): mantle made entirely of Fo90 olivine without melt extraction and solid phase transition, "+crust+k_{rad}+phase changes" (blue): pyrolitic mantle with the effects of oceanic crust, radiative thermal conductivity, melt extraction, and solid phase transition, "+thermal cracking" (green): with reduction in effective thermal expansivity caused by thermal cracking, "+internal heating" (orange): with the effect of radiogenic heating equivalent to 9 TW for the convecting mantle, and "+secular cooling" (red): with the effect of secular cooling at the rate of 100 K Gyr^{-1}. Observed subsidence rate ($\sim$320$-$330 m Ma^{-1}) is shown in gray.

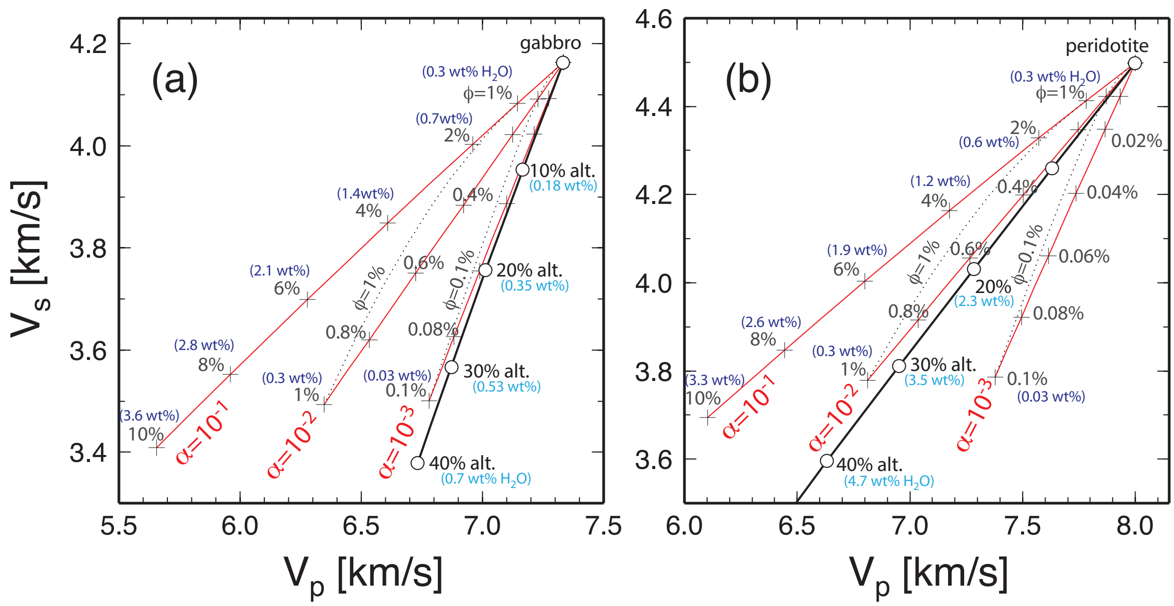

Figure 3: (a) Effects of alteration (solid line with open circles) and crack porosity (red lines with crosses) on the seismic velocities of gabbbro, after Korenaga (2017a). Numbers next to symbols denote the degree of alteration or porosity. For crack porosity, the cases of three different aspect ratios (10^{-1}, 10^{-2}, and 10^{-3}) are shown. Numbers in parentheses are equivalent water contents. Dotted lines connecting different aspect ratios (but with the same porosity) illustrate the effect of varying the aspect ratio. (b) Effects of serpentinization and crack porosity on the seismic velocities of peridotite. For serpentinite, data for lizardite serpentinites are used here; this is appropriate when the mantle just below the normal oceanic crust near subduction zone is colder than 300 °C. For higher temperatures, antigorite forms instead, and its effect on seismic velocities follows the same trend of that for lizardite; the only difference is the corresponding degree of alteration, and a factor of $\sim$2.5 should be multiplied to convert from lizardite values (e.g., V_p of $\sim$6.6 km s^{-1} and V_s of $\sim$3.6 km s^{-1} corresponds to 40 % alteration in case of lizardite, but to 100 % alteration in case of antigorite). See Korenaga (2017a) for further details.

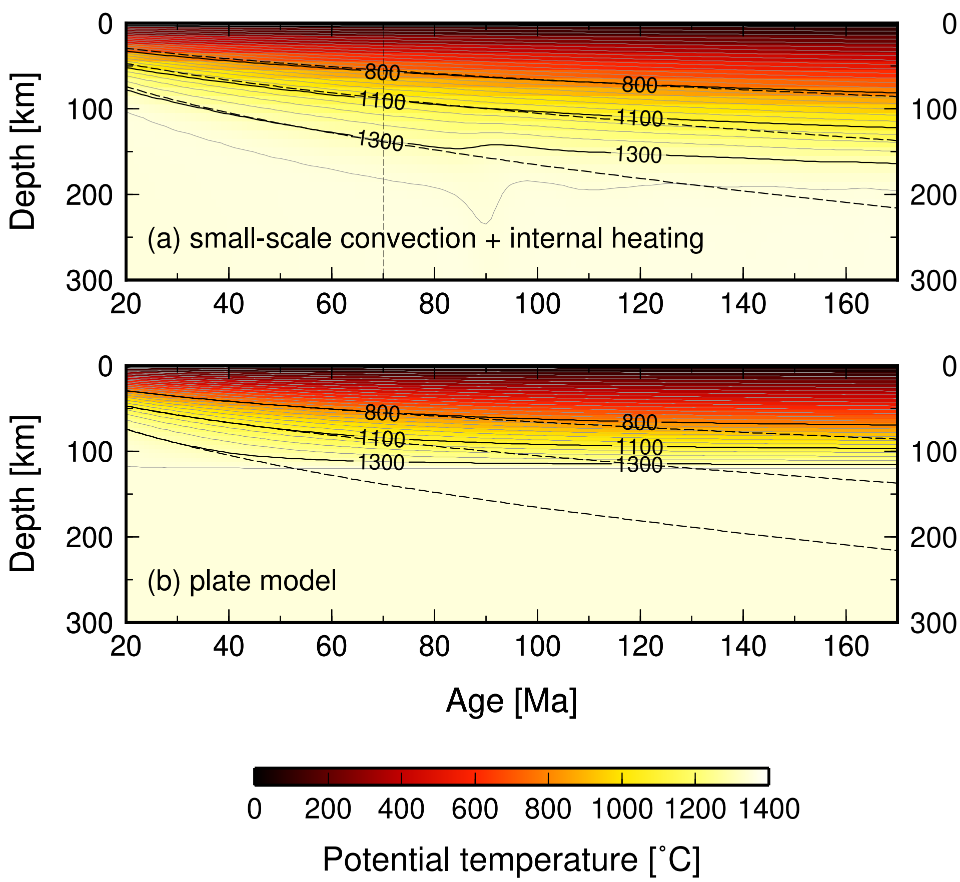

Figure 4: (a) Thermal evolution of oceanic upper mantle based on numerical modeling, after averaging out-of-plane (i.e., ridge-parallel) variations. Initial mantle potential temperature is set to 1350 °C. In this model, small-scale convection initiates at the age of 70 Ma, and the assumed amount of radiogenic heating corresponds to 13 TW for the convecting mantle. Gray contours are drawn at every 50 K, and isotherms of 800 °C, 1100 °C, and 1300 °C are shown in solid. Also shown are isotherms according to simple half-space cooling (dashed). After Korenaga (2015b). (b) Same as (a) but with the thermal evolution according to the plate model with the plate thickness of 120 km.

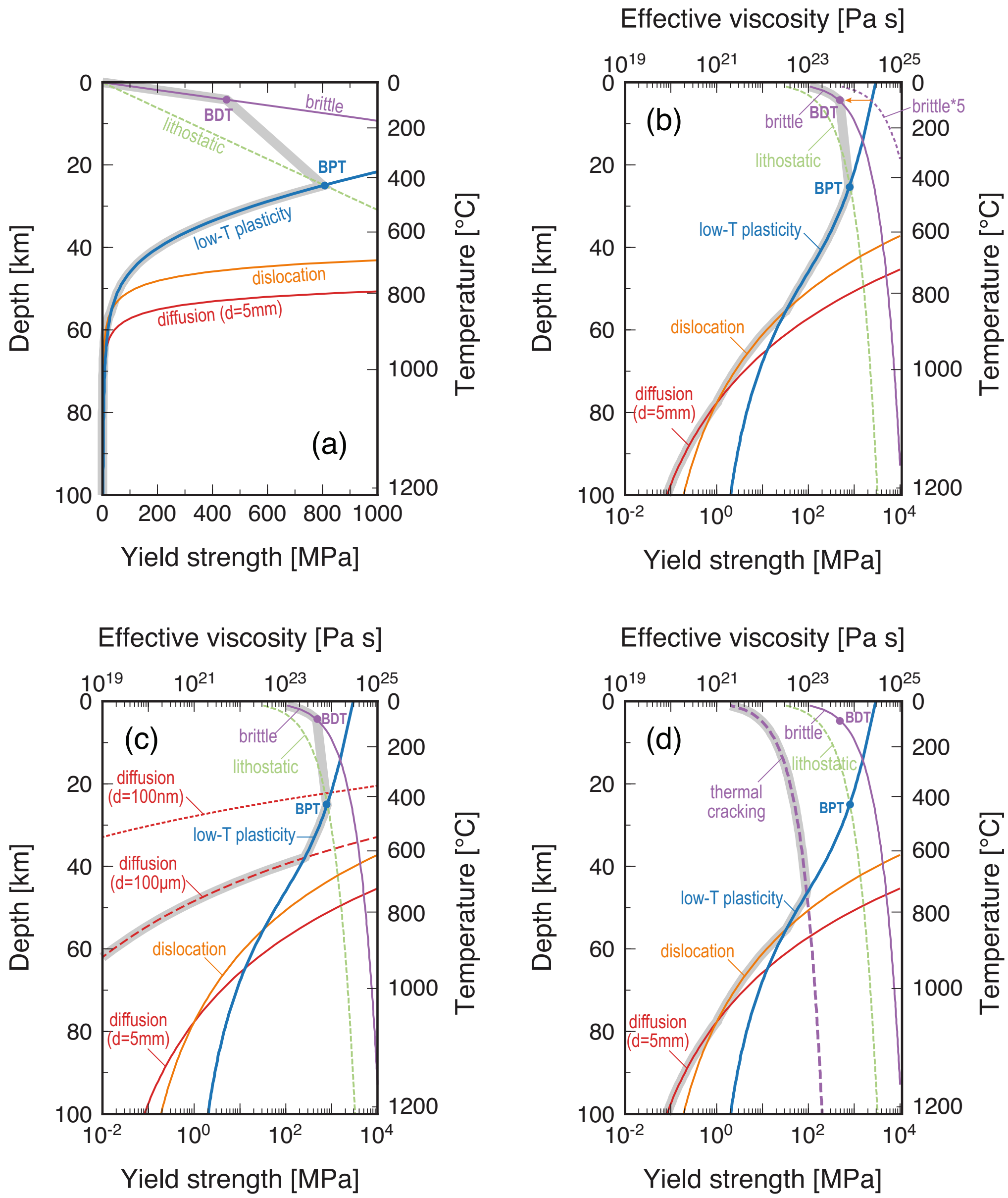

Figure 5: Hypothetical yield strength profiles for present-day oceanic lithosphere at the seafloor age of 60 Ma. Only the top 100 km is shown, and the assumed thermal structure, based on half-space cooling with the initial temperature of 1350 °C, is indicated on the right axis. Yield strength is calculated assuming the geological strain rate of 10^{-15} s^{-1}, so the yield strength of 1 GPa corresponding to the effective viscosity of 10^{24} Pa s. The effect of thin crustal layer is ignored, and deformation mechanisms considered here include: (1) diffusion creep with the activation energy of 300 kJ mol^{-1} and the grain size exponent of 2, with the reference viscosity of 10^{19} Pa s at 1350 °C and the grain size of 5 mm, (2) dislocation creep with the activation energy of 600 kJ mol^{-1} and the stress exponent of 3, with the reference viscosity of 10^{19} Pa s at 1350 °C and the deviatoric stress of 0.1 MPa, (3) low-temperature plasticity based on the reanalysis of the experimental data of Mei et al. (2010) by Jain et al. (2017), with the exponents of $p = 1$ and $q = 2$, (4) brittle strength with the friction coefficient of 0.8 under optimal thrust faulting, and (5) brittle-ductile and brittle-plastic transitions (Kohlstedt et al. 1995). (a) Yield strength profiles in the linear stress scale. Lithostatic stress is shown in dashed green, and yield stress envelope in gray. (b) Same as (a) but in the log stress scale. (c) Same as (b) but with diffusion creep with two different grain sizes (100 μm and 100 nm). (d) Same as (b) but with thermal cracking, assuming the effective friction coefficient of 0.03 (Korenaga 2011a).

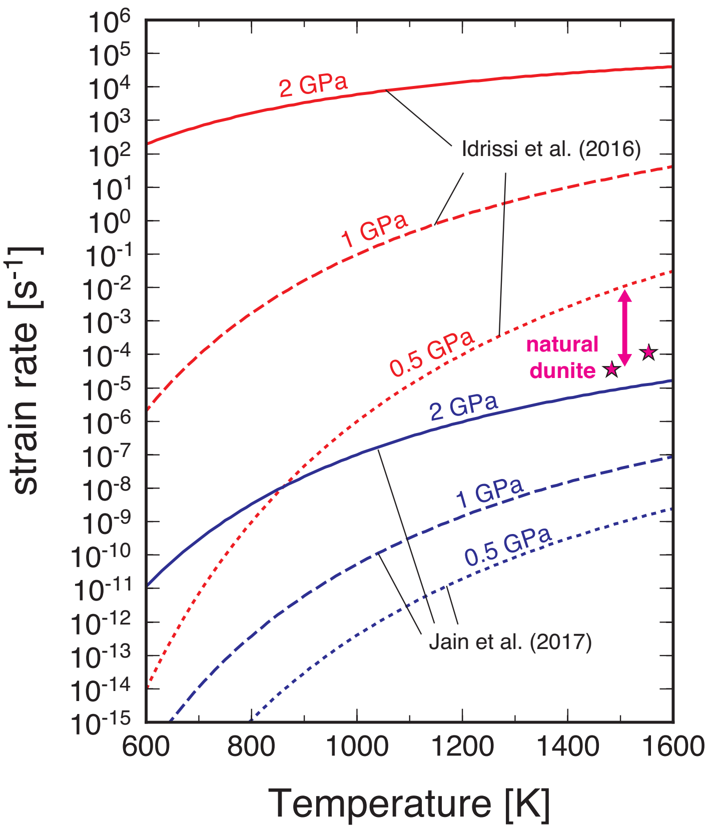

Figure 6: (a) Predicted strain rates as a function of temperature using the flow laws of Idrissi et al. (2016) (red) and Jain et al. (2017) with p=1 and q=2 (blue), for three different stresses: 0.5 GPa (dotted), 1 GPa (dashed), and 2 GPa (solid). The confining pressure is set to 6 GPa for the latter flow law. Stars denote the deformation data of natural dunite with ∼900 μm grain size (Chopra and Paterson 1984): stresses are 0.485 GPa for the 1483 K data and 0.481 GPa for the 1553 K data.

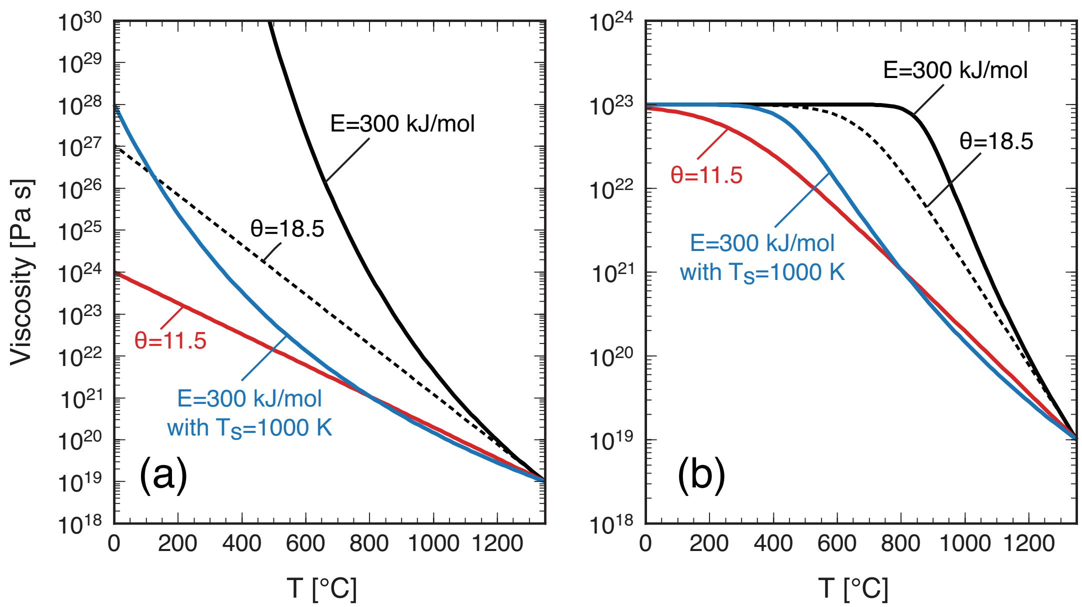

Figure 7: A few examples of temperature-dependent viscosity. In all cases, the reference viscosity is set to 10^{19} Pa s at the temperature of 1350 °C. (a) Purely temperature-dependent viscosity. Arrhenius-type dependence (equation (12)) with the activation energy of 300 kJ mol^{-1} and the surface temperature of 273 K (black) and 1000 K (blue), and linear-exponential dependence (equation (14)) with the Frank-Kamenetskii parameter of 18.5 (black-dashed) and 11.5 (red). (b) Harmonic mean of temperature-dependent viscosity and the viscosity of 10^{23} Pa s (equation (16)). The viscosity of 10^{23} Pa s corresponds to the yield stress of 100 MPa with the strain rate of 10^{-15} s^{-1}. Line legend is the same as in (a).